Jaypee Gold Standard Mini Atlas Series

Emergency Imaging

Jaypee Gold Standard Mini Atlas Series

Emergency Imaging

D Karthikeyan DMRD DNB
Consultant Radiologist
Bharat Heart Scans
Chennai

Deepa Chegu DMRD
Consultant Radiologist
Bharat Scans
Chennai

JAYPEE BROTHERS
MEDICAL PUBLISHERS (P) LTD
New Delhi

Published by

Jitendar P Vij
Jaypee Brothers Medical Publishers (P) Ltd
EMCA House, 23/23B Ansari Road, Daryaganj
New Delhi 110 002, India
Phones: +91-11-23272143, +91-11-23272703, +91-11-23282021, +91-11-23245672 Rel: 32558559
Fax: +91-11-23276490, +91-11-23245683
E-mail: jaypee@jaypeebrothers.com Visit our website: www.jaypeebrothers.com

Branches

- 2/B, Akruti Society, Jodhpur Gam Road Satellite, **Ahmedabad** 380 015
  Phones: +91-079-26926233, Rel: +91-079-32988717, Fax: +91-079-26927094
  e-mail: ahmedabad@jaypeebrothers.com
- 202 Batavia Chambers, 8 Kumara Krupa Road, Kumara Park East, **Bengaluru** 560 001
  Phones: +91-80-22285971, +91-80-22382956, Rel: +91-80-32714073
  Fax: +91-80-22281761 e-mail: bangalore@jaypeebrothers.com
- 282 IIIrd Floor, Khaleel Shirazi Estate, Fountain Plaza, Pantheon Road, **Chennai** 600 008
  Phones: +91-44-28193265, +91-44-28194897, Rel: +91-44-32972089
  Fax: +91-44-28193231 e-mail: chennai@jaypeebrothers.com
- 4-2-1067/1-3, 1st Floor, Balaji Building, Ramkote Cross Road, **Hyderabad** 500 095
  Phones: +91-40-66610020, +91-40-24758498, Rel:+91-40-32940929
  Fax:+91-40-24758499, e-mail: hyderabad@jaypeebrothers.com
- No. 41/3098, B & B1, Kuruvi Building, St. Vincent Road, **Kochi** 682 018, Kerala
  Phone: +91-0484-4036109, +91-0484-2395739, +91-0484-2395740
  e-mail: kochi@jaypeebrothers.com
- 1-A Indian Mirror Street, Wellington Square, **Kolkata** 700 013
  Phones: +91-33-22451926, +91-33-22276404, +91-33-22276415, Rel: +91-33-32901926
  Fax: +91-33-22456075, e-mail: kolkata@jaypeebrothers.com
- 106 Amit Industrial Estate, 61 Dr SS Rao Road, Near MGM Hospital, Parel, **Mumbai** 400012
  Phones: +91-22-24124863, +91-22-24104532, Rel: +91-22-32926896
  Fax: +91-22-24160828, e-mail: mumbai@jaypeebrothers.com
- "KAMALPUSHPA" 38, Reshimbag, Opp. Mohota Science College, Umred Road
  Nagpur 440 009 (MS) Phones: Rel: 3245220, Fax: 0712-2704275
  e-mail: nagpur@jaypeebrothers.com

Jaypee Gold Standard Mini Atlas Series: Emergency Imaging

First Edition: **2007**

ISBN 81-8061-942-7

Typeset at JPBMP typesetting unit
Printed at Ajanta Offset

Preface

Contrast-enhanced spiral CT and high field MRI has revolutionized the work-up and diagnosis of the trauma and emergency patient. State-of-the-art CT and MRI technology with multislice capabilities allows for rapid breath-hold scanning, permitting greater coverage with greater spatial detail. CT may be performed in hemodynamically stable patients in whom injury is suspected in much less time than in the recent past with greater accuracy and diagnostic confidence.

These capabilities have led to a dramatic decrease in surgical exploration for often minor injuries, improved triage by presenting the total spectrum of injuries, permitted recognition of clinically unanticipated injuries, and fostered earlier discharge of patients without significant injury with a high level of confidence. These influences have, in turn, led to decrease in costs of patient management and, most likely, improved overall clinical outcomes.

It is our hope that this new mini series in a pictorial review format will help the postgraduate students and emergency room physicians.

D Karthikeyan
Deepa Chegu

Contents

1. Traumatic Brain Injuries

TRAUMATIC BRAIN INJURIES

Closed head injury
Penetrating head injury
Compressive head injury
Concussion
Epidural hematoma
Subdural hematoma
Subdural hygroma
Contusion
Coup and contrecoup
Laceration
Diffuse axonal injury
Hypoxia
Edema
Transtentorial herniation
Cerebellar herniation
Post-traumatic epilepsy

Emergency Imaging

Contact injuries	*Acceleration injuries*
Skull deformation injuries, local i. Skull fracture, linear or depressed ii. Extradural hematoma iii. Coup contusions	Surface strain i. Subdural hematoma ii. Contrecoup contusion iii. Intermediate coup contusion
Remote Vault and basal skull fractures	Deep strain Concussive syndromes Diffuse axonal injury.
Shock wave injures Contrecoup contusion ICH	

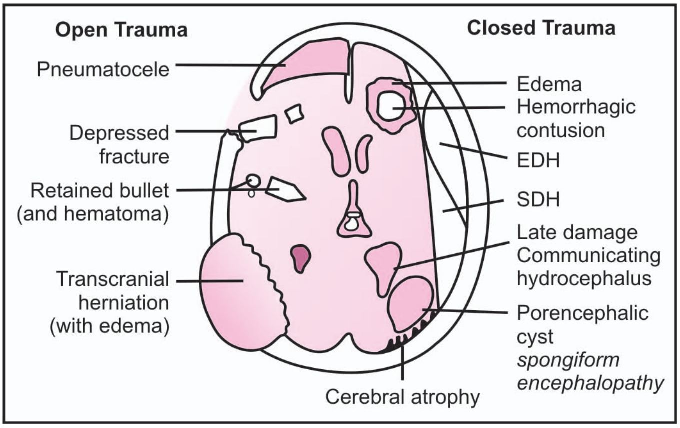

(2)

HYPERACUTE EDH

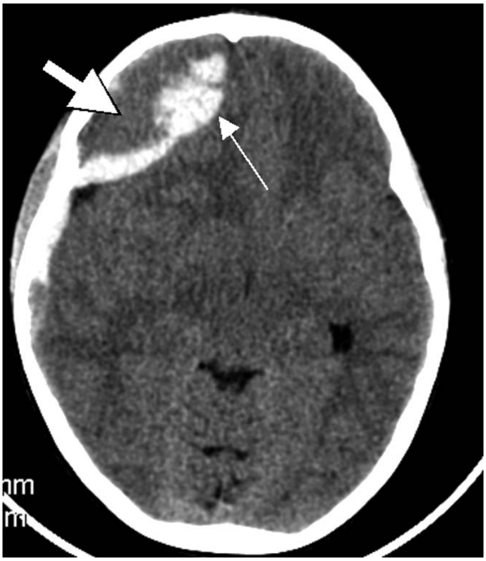

Axial NECT shows a right frontal convex extra axial lesion showing rim of hyperdensity(thin arrow) with a large iso dense component (short arrow) suggesting hyperacute on going bleed. Note the cortical buckling.

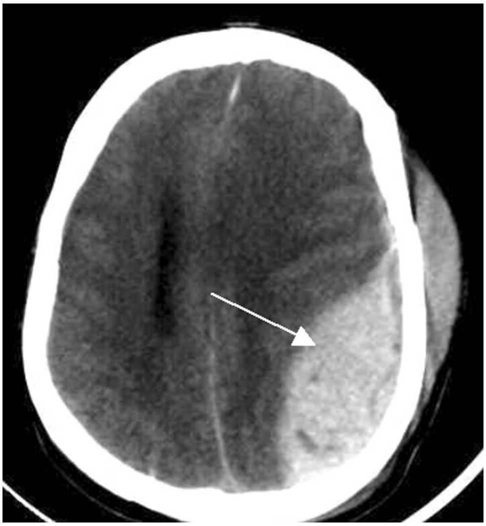

Axial NECT showing an acute left parietal EDH.

CHRONIC SDH

Axial CECT shows a right frontoparietal concave mixed dense extra axial collection (thin arrow) causing cortical buckling and mid line shift, note the displaced ventricles with subfalcine herniation (thick arrow). Layering of the collection is classical finding of chronicity.

ACUTE SDH

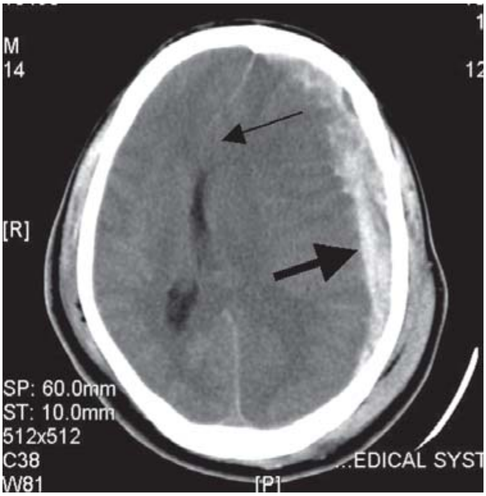

Axial NECT showing left frontoparietal concave hyperdense collection (thick arrow) with midline shift and subfalcine herniation (thin arrow).

CONTUSION

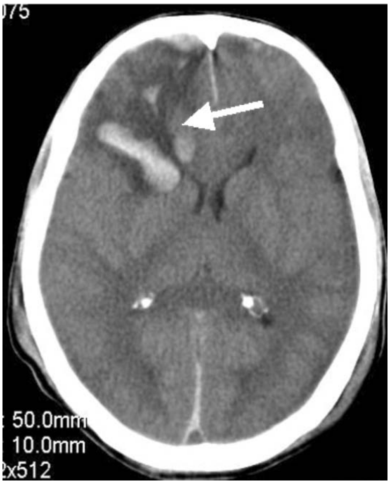

Axial NECT showing right frontal hemorrhagic contusion, note the mixture of high and low attenuation lesions (arrow).

DIFFUSE AXONAL INJURY

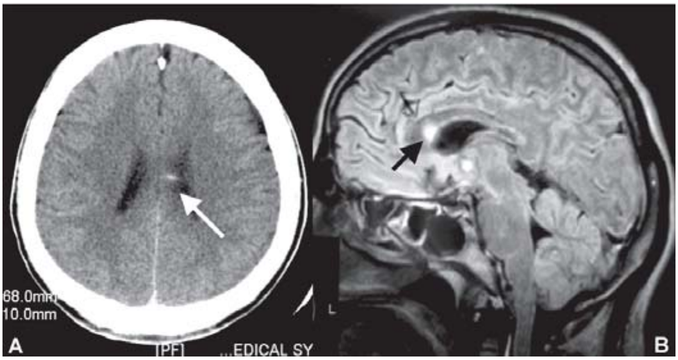

Figure A axial NECT showing a focal high attenuation in the region of body of callosum (arrow). Figure B sag t2 W MRI showing a focal high signal intensity in the genu of callosum.

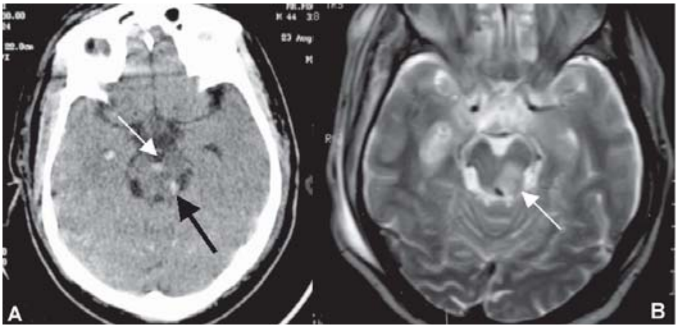

Figure A axial NECT showing punctuate bleed in the left cerebral peduncle along with interpeduncular SAH (arrows). Axial t2 W MRI showing high signal intensity in the left peduncle (arrow).

Classification of DAI

Stage I: Involves the parasagittal regions of the frontal lobes, periventricular temporal lobes and less likely the parietal and occipital lobes, internal and external capsules, and cerebellum.

Stage II: Involvement of the corpus callosum, in addition to the white matter areas in stage I.

Stage III: Involves the areas associated with stage II, with the addition of brainstem involvement.

PNEUMOCEPHALUS

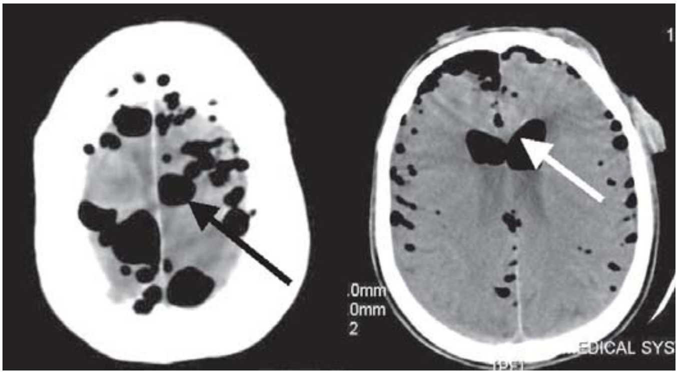

Axial NECT showing multiple air pockets in the parenchyma, intraventricular region and in the frontal subdural space (arrows).

POST-TRAUMATIC INFARCT

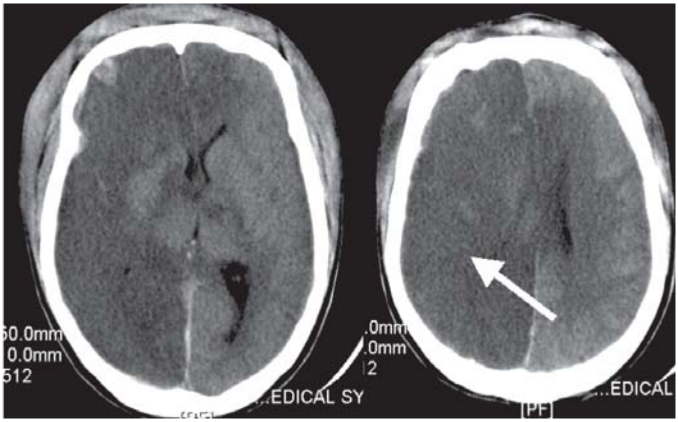

Axial NECT in a patient who had sustained a motor vehicle accident showing right hemispherical infarct (arrow). Post-traumatic infarcts occur either due to spontaneous ICA dissection or thrombosis due to shearing injury.

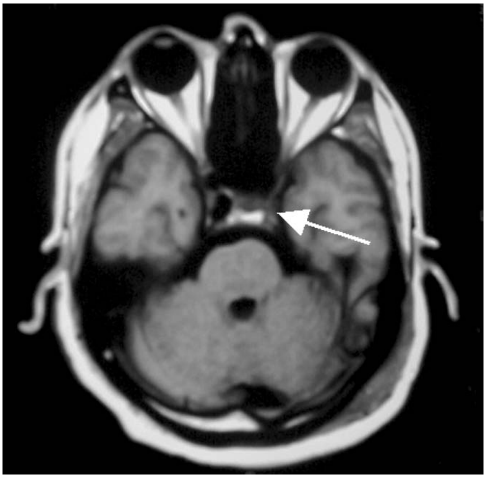

Axial t1W MRI shows loss of normal left ICA flow void (arrow) case of post-traumatic occlusion.

CRANIAL FRACTURES

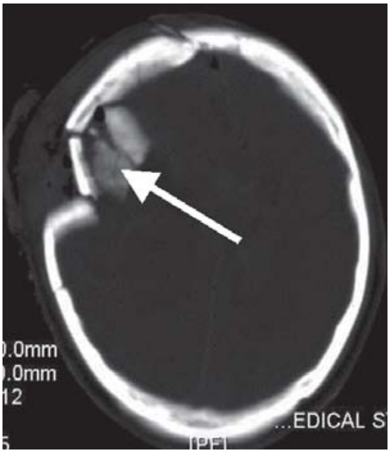

Axial NECT in bone window showing a left frontal comminuted depressed fracture (arrow).

REVERSAL SIGN –SIGN OF HYPOXIA

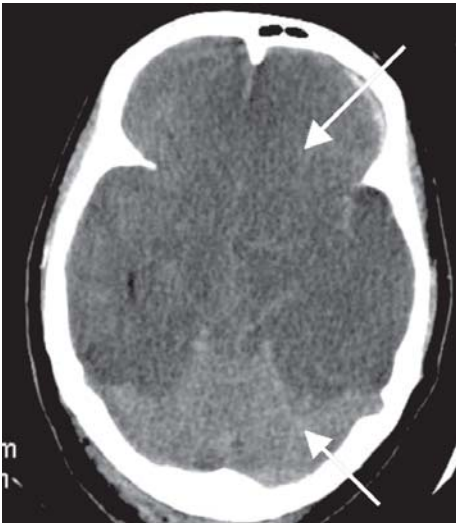

Axial CECT shows diffuse hypodensity of the supratentorial cerebral hemisphere with cerebellum showing normal attenuation (arrows).

CAROTICOCAVERNOUS FISTULA

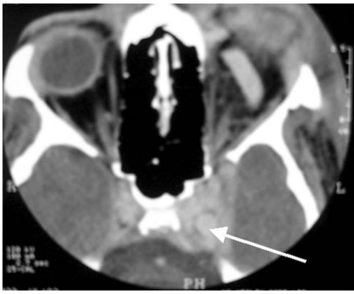

Axial CECT shows left orbital proptosis with distended left cavernous sinus and dilated superior ophthalmic vein (arrow).

Usually caused by trauma or spontaneous rupture of the cavernous ICA. Routes of drainage will include superior ophthalmic vein, petrosal sinus, cortical veins, contralateral sinus.

2. Non- traumatic Brain Emergencies

ANEURYSM

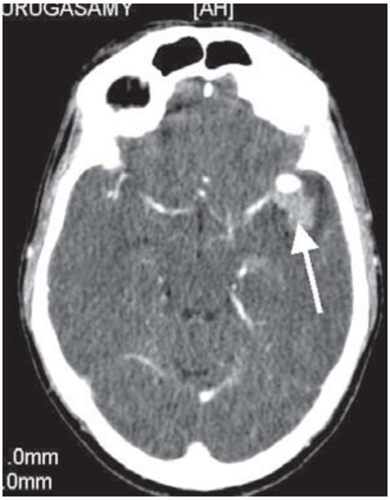

Axial CECT showing a left middle cerebral artery aneurysm with bleed (arrow).

AVM

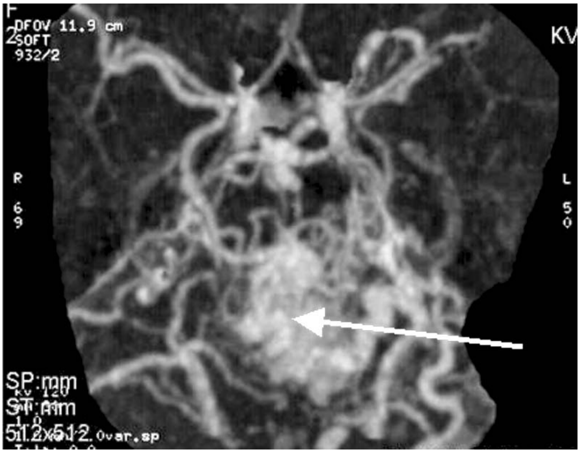

3d MIP reconstruction showing a large posterior fossa AVM with feeders from PCA draining into the left transverse sinus (arrow).

INTRACEREBRAL BLEED

Potential mechanisms and factors associated with intracerebral hemorrhages.

- Amyloid angiopathy
- Arterial hypertension
- Arterio-venous malformation
- Arterial aneurysm (congenital or mycotic)
- Cerebral vasculitis
- Cerebral venous infarction
- Cocaine
- Coagulopathy
- Hemorrhagic conversion of ischemic stroke
- Secondary hemorrhage into primary or secondary brain neoplasm
- Stimulant drugs

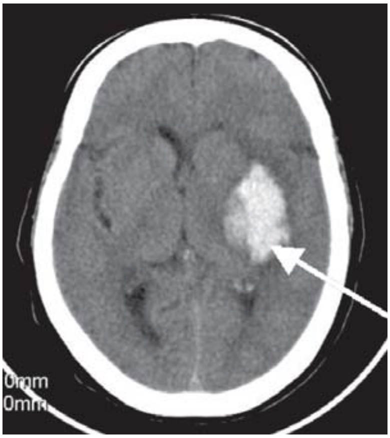

Axial NECT showing a left gangliocapsular acute hematoma.

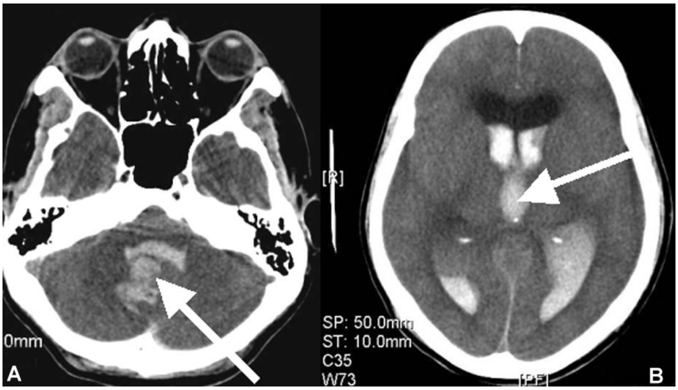

Axial NECT showing acute vermian bleed (Fig. A) with intraventricular extension causing obstructive hydrocephalus (Fig. B).

Axial NECT showing acute left corona bleed with intraventricular extension (arrow).

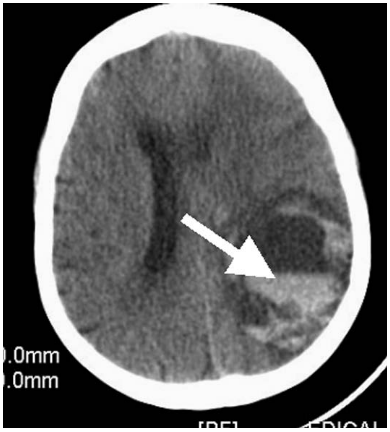

Axial NECT showing left posterior parietal low hematocrit hematoma, note the fluid fluid level which is seen classically in these bleeds which are seen in patients with renal failure or coagulation derangement.

- **Acute (0-2 days) — hyperdense**
- **Subacute (3-14 days) — isodense**
- **Chronic (>14 days) — hypodense**

CEREBRAL VENOUS SINUS THROMBOSIS

Axial CECT showing bilateral subcortical bleeds in the frontoparietal regions (arrow, Fig. A). Figure B shows the nonenhancing superior sagittal sinus suggestive of thrombosis (arrow).

STRAIGHT SINUS THROMBOSIS

Axial NECT showing hyperdense straight sinus due to thrombosis (arrow) causing bithalamic infarcts.

ABSCESS

Axial CECT showing right temporal conglomerate low dense lesion showing smooth enhancing capsule in a boy with cyanotic heart disease classical findings of a pyogenic abscess.

COLLOID CYST

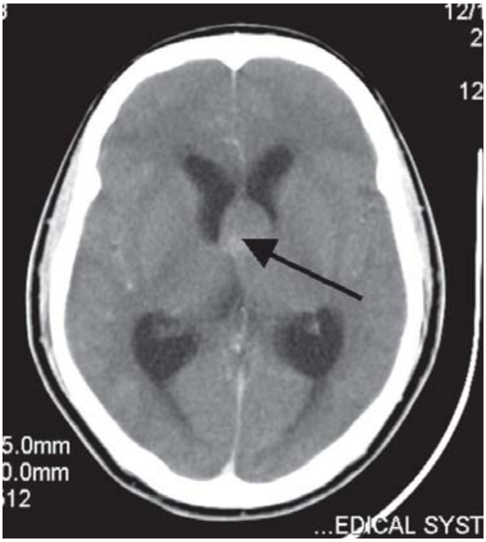

Axial CECT showing a hyperdense lesion in the left foramen of monro causing obstructive hydrocephalus. Patients present with headache and giddiness.

MEDULLOBLASTOMA

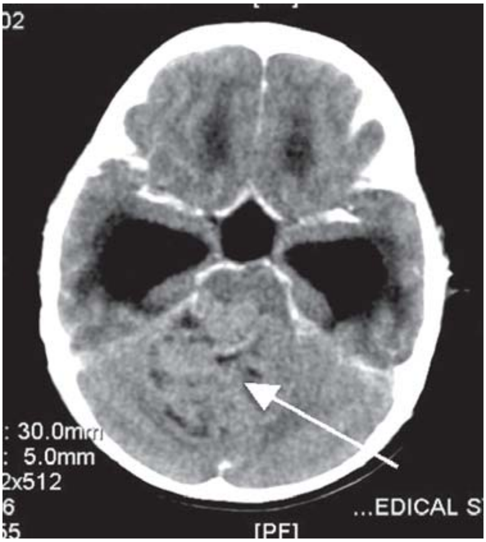

Axial CECT showing a variegated posterior fossa mass with obstructive hydrocephalus. Patient presents with features of raised ICT.

POSTERIOR REVERSIBLE ENCEPHALOPATHY

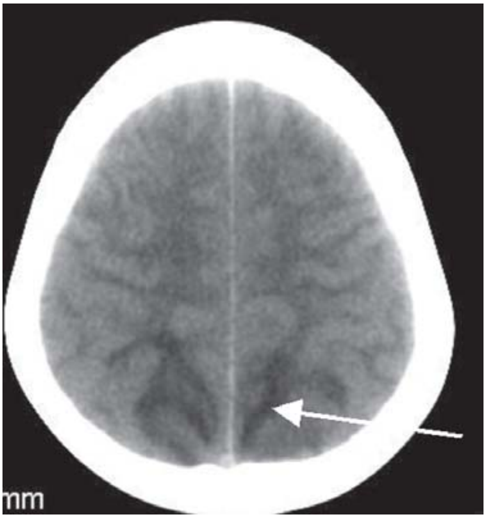

Axial CECT showing bilateral posterior parietal hypodensity in a young girl with hypertension due to acute nephritis. This is caused due to break down of the blood-brain barrier with transudation of fluid due to transient loss of auto-regulatory mechanisms.

DENSE MCA SIGN

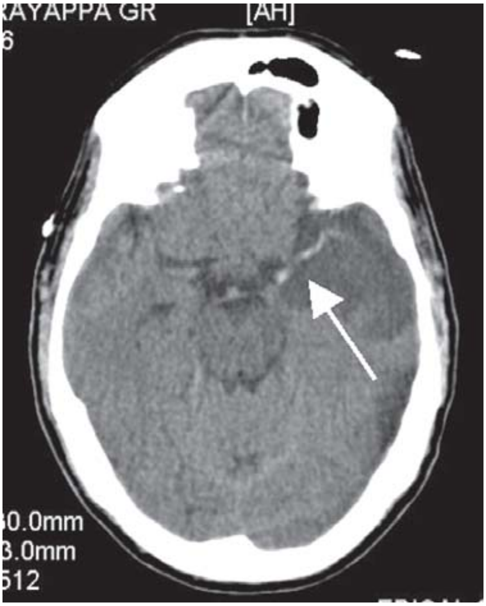

Axial NECT showing hyperdense left MCA due to acute thrombus (arrow). Note the adjacent insular hypodensity due to acute infarct.

PROGRESSION OF AN INFARCT

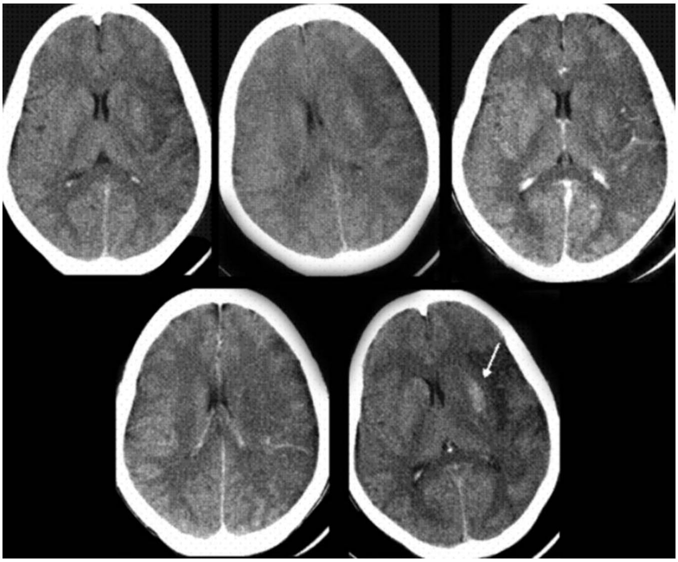

Axial NE and CECT taken over a period of 8 days shows the transition of a left MCA infarct from an acute to subacute pattern with hemorrhagic transformation of the left lentiform nucleus.

LEFT MCA PROXIMAL OCCLUSION

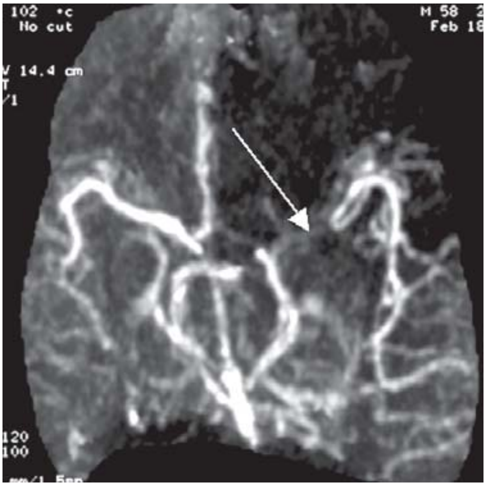

3D MIP cerebral angiogram shows proximal left MCA m1, m2 segment occlusion.

BASILAR ARTERY OCCLUSION

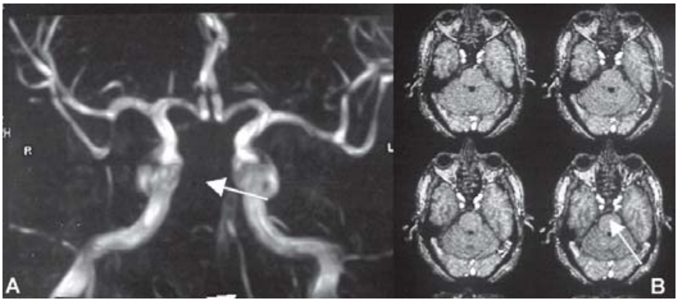

MR 3D TOF angiogram shows absent flow in the basilar artery. Figure B shows source images which confirm lack of flow in the distal basilar artery (arrow).

DURETS HEMORRHAGE

Axial NECT showing linear hyperdensities in the pons caused due rupture of the pontine perferator vessels due to downward herniation.

3. Traumatic Chest Injuries

Require Immediate Intervention

- Tension pneumothorax
- Open pneumothorax
- Disruption of major airway
- Cardiac tamponade
- Massive hemothorax
- Traumatic air embolism
- Flail chest

Injuries with Potential for Threatening Survival

- Lung contusion
- Other pulmonary parenchymal injuries
- Myocardial contusion
- Aortic rupture
- Esophageal disruption
- Diaphragmatic rupture
- Rib fractures

- Simple hemopneumothorax
- Traumatic asphyxia

Long-term Sequelae

- Clotted hemothorax
- Empyema
- Phrenic nerve palsy
- Pericardial complications
- Fistulae
- Diaphragmatic hernia
- Chylothorax

Others

- Sternal, clavicular, scapular injuries
- Subcutaneous emphysema

PNEUMOTHORAX

Accumulation of air in the pleural space.

Common causes are blunt/penetrating trauma, iatrogenic and spontaneous (underlying lung diseases). There are 3 types:

Type 1—closed, intact thoracic cage

Type 2—open, sucking chest wound

Type 3—tension, free ingress with little egress

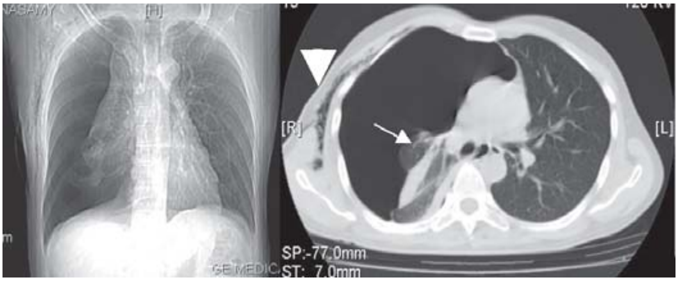

Digital scanogram and axial CT showing collapsed right lung (thin arrow) due to gross pneumothorax. Note the subcutaneous emphysema (short arrow).

PNEUMOTHORAX WITH PULMONARY CONTUSION

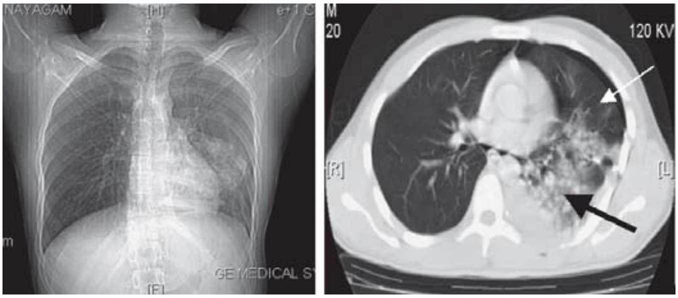

Digital scanogram and axial CT showing rim of left pneumothorax (thin arrow) with pulmonary parenchymal alveolar opacities suggestive of contusion.

PNEUMOMEDIASTINUM

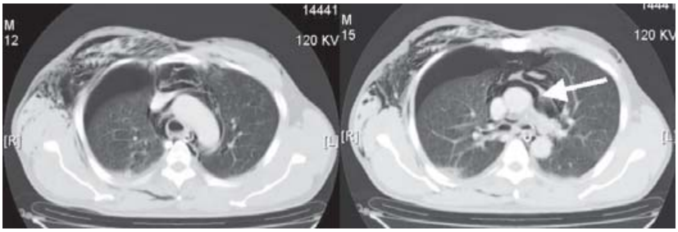

Axial NECT showing right pneumothorax, right subcutaneous emphysema and air within the mediastinal fat planes (arrow).

LUNG CONTUSION

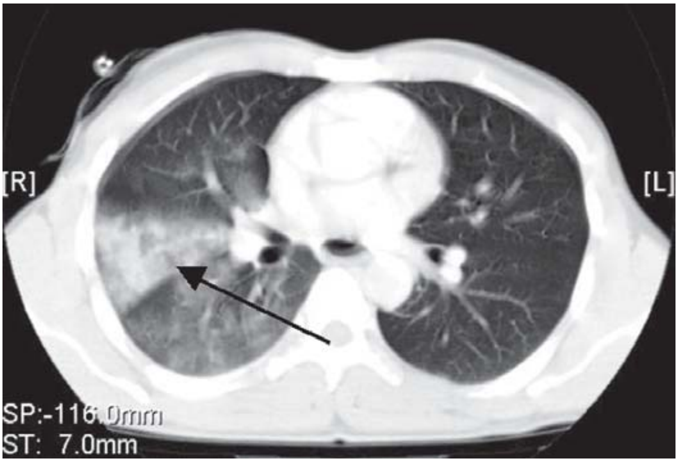

Axial NECT showing right upper lobe posteriror and lower lobe superior segment parenchymal consolidation with alveolar opacity typical of contusion in the acute setting.

Contusions appear as nonsegmental coarse illdefined amorphous opacities usually located posteriorly overlying the rib fractures. Classically seen as nonsegmental pulmonary infiltrates—occur within 12-24 hours of injury.

PULMONARY LACERATION

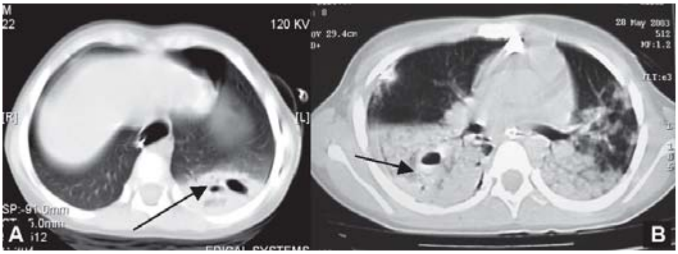

Axial NECT showing left lower lobe peripheral laceration (arrow Fig. A), Figure B shows bilateral lower lobe contusion with right laceration seen as an oval lucency.

Post-traumatic cysts, pseudocysts, or pneumatoceles are cavitary lesions within the lung parenchyma filled with fluid, blood, of laceration.

Pulmonary laceration is defined as air filled lucencies surrounded by lung parenchyma as seen on CT. Pulmonary lacerations are classified into 4 types based on CT parameters—

Type 1—intraparenchymal air filled cavity

Type 2—air filled cavity in the paravertebral parenchyma

Type 3—linear lucency seen adjacent to a fractured rib

Type 4—pleuro-pulmonary adhesion.

POST-TRAUMATIC ARDS

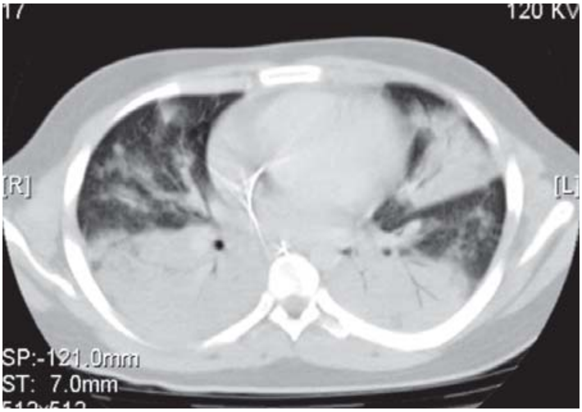

Axial NECT showing bilateral multifocal consolidations in a patient who had sustained left femur and right foot fractures.

DIAPHRAGMATIC INJURY

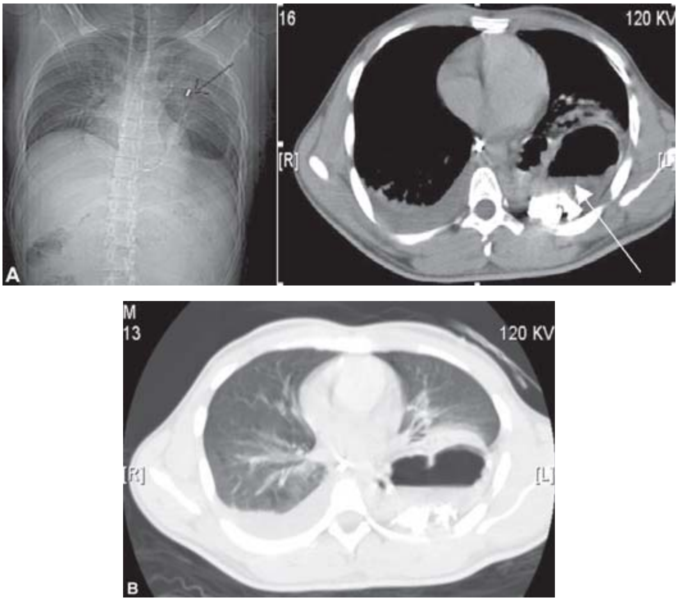

Digital scanogram and axial CT in mediastinal and lung window showing transthoracic herniation of the stomach due to diaphragmatic tear. Note the high placed stomach in Figure A, Figure B shows the oral contrast injected via the Ryle's tube reaching the stomach.

INJURY TO AORTA

Deceleration forces can cause marked shearing stresses particularly where a structure changes from being relatively fixed to relatively unsupported, such a zone occurs in the aortic isthmus in the region of attachment of ligament arteriosum. Ninety-five percent of the aortic injuries are encountred at the aortic isthmus level.

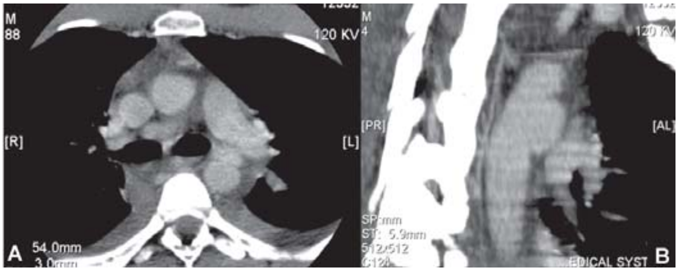

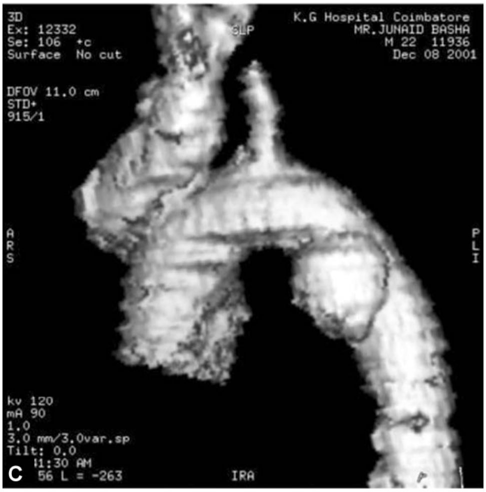

Axial CECT with sagittal and 3d SSD reformation shows a saccular aneurysm in the region of aortic isthmus. Patient had sustained a motor vehicle accident.

4. Non-traumatic Chest Emergencies

PENETRATING ATHEROMATOUS ULCER

Axial CECT showing an eccentric intimal ulcer. Patient usually presents with chest pain and are evaluated for CAD.

PULMONARY EMBOLISM

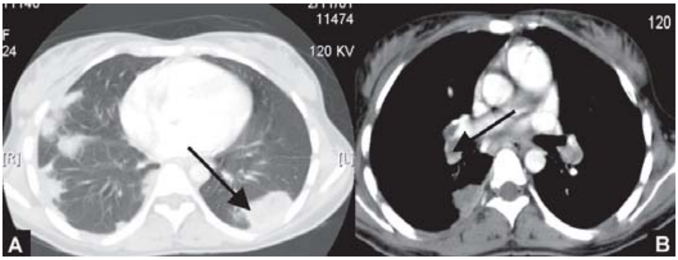

Axial CECT in lung and mediastinal window show classical pulmonary infarcts seen as wedge shaped pleural based lesions (arrow in Fig. A) due to bilateral segmental pulmonary embolus (arrow in Fig. B).

RASMUSSENS ANEURYSM

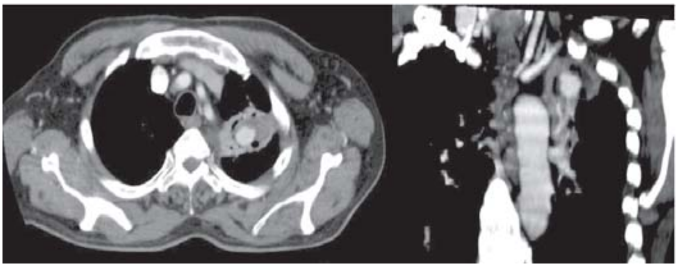

Axial CECT and coronal reformat images show a left upper lobe cavity with an enhancing focus within.

AORTIC DISSECTION

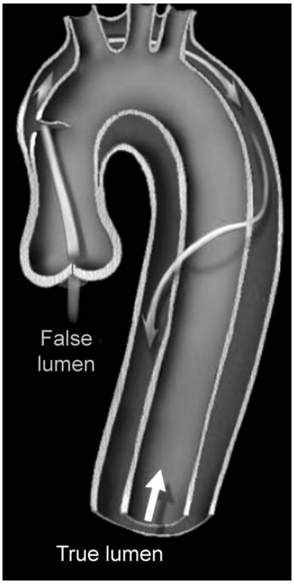

(For colour version see Fig. 1, Plate 1)

Type I: Originates in the ascending aorta, propagates at least to aortic arch often beyond it distally into the descending thoracic and abdominal aorta.

Type II: Originates in and confined to ascending aorta.

Type III: Originates in the descending aorta and extends distally down the aorta or rarely retrograde into the arch.

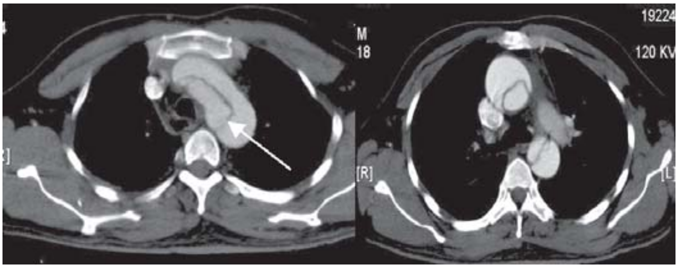

Axial CECT showing the intimal flap in the arch, ascending and descending aorta (arrow) type 1 dissection.

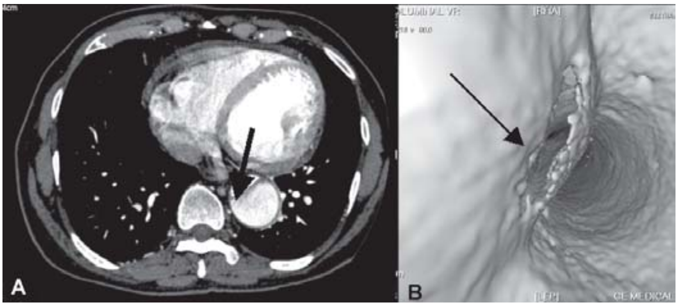

Axial CECT showing dissecting flap in the descending aorta, Figure B shows the endoluminal view at the entry point of the flap.

CONSOLIDATION

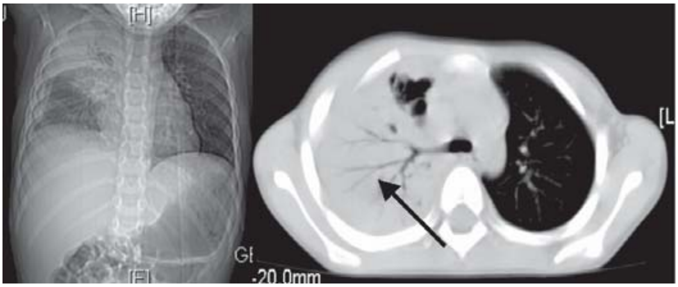

Scanogram and axial CT showing right upper lobe consolidation, note the classical air bronchogram.

ARDS DUE TO TOXIC GAS INHALATION

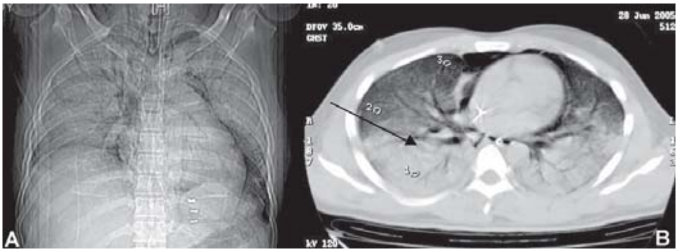

Digital scanogram with axial CT shows bilateral consolidative changes. Note the gravity dependent gradient (Fig. B) showing denser changes in the bases (arrow).

PULMONARY EDEMA

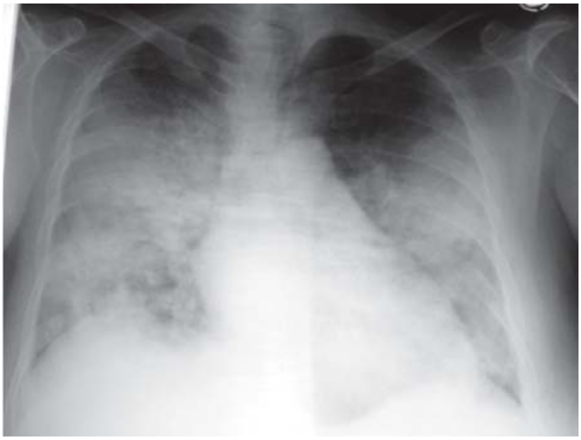

X-ray chest showing the classical bats wing appearance of pulmonary edema.

Radiological sign	*Cardiogenic*	*Renal*	*Capillary injury*
Heart shape	L-sided enlargement	R & L enlargement	Normal
Vascular pedicle width (SV)	+	++	Normal
Pulmonary blood distribution	Balanced or inverted	Balanced	Normal
Pulmonary blood volume	Normal or +	++	Normal
Septal lines	++	+	No
Peribronchial & vessel cuffing	+	+	No
Air bronchogram	+	+	++
Lung opacity distribution	Central & peripheral	Central	Peripheral & central
Pleural effusion	++	+	Uncommon
Soft-tissue chest wall	+	++	Normal

5. Non-traumatic Abdominal Emergencies

CAUSES

a. The peritoneal cavity
   - Ascites
   - Peritonitis
   - Abdominal abscess

b. Liver and biliary tract
   - Jaundice: obstructive and non-obstructive
   - Cholecystitis

c. Pancreatitis

d. Urinary tract
   - Urinary stones
   - Infection
   - Pyelonephritis
   - Renal abscess

e. Adrenal hemorrhage

f. Gastrointestinal tract
   - Gastrointestinal hemorrhage
   - Bowel obstruction

- Bowel infarction
- Bowel infection
- Appendicitis
- Diverticulitis
- Infectious enteritis and colitis

g. Epiploic appendagitis

h. Inflammatory bowel disease
- Crohn disease
- Ulcerative colitis
- CT protocols in patients with acute abdomen tailored to the clinical working diagnosis.

No intravenous contrast	Ureteral stone, intra-abdominal bleeding, hematoma
No oral contrast	Ureteral stone, vascular disease, small bowel obstruction, pancreatitis
Negative oral contrast (water)	Gastroduodenal ulcer, intraductal gallstone
Rectal contrast (optional)	Appendicitis, diverticulitis
Increased flow rate of IV contrast	Vascular disease, hemorrhage, bowel ischemia, renal infarct
Delayed acquisition (> 3 min)	Pyelonephritis
Narrow collimation	Ureteral stone, intraductal gallstone, vascular disease
Small recon. interval (≤ 3 mm)	As with narrow collimation, + small bowel disease

GIST TUMORS WITH HEMORRHAGE

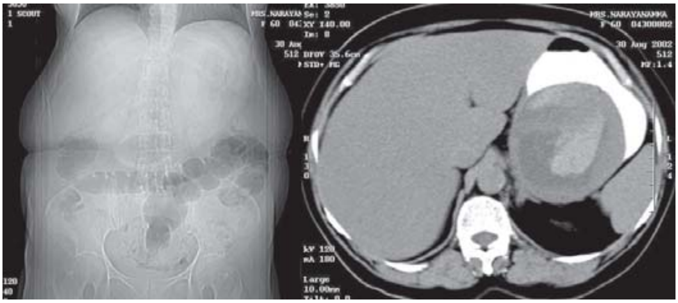

Digital scanogram and axial CECT showing a large encapsulated mass indenting the gastric fundus lesion shows central area of necrosis with hyperdense areas of hemorrhage. Patient presented with hematemesis.

IRREDUCIBLE HERNIA WITH SUBACUTE BOWEL OBSTRUCTION

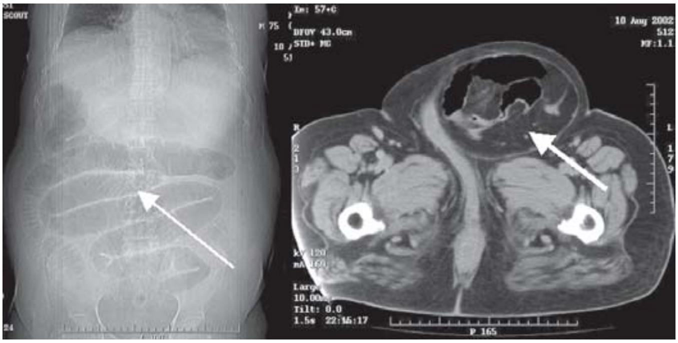

Digital scanogram showing dilated bowel loops. Axial CECT at the pubic level shows a large inguinoscrotal hernia with bowel and mesentery as content.

VOLVULUS

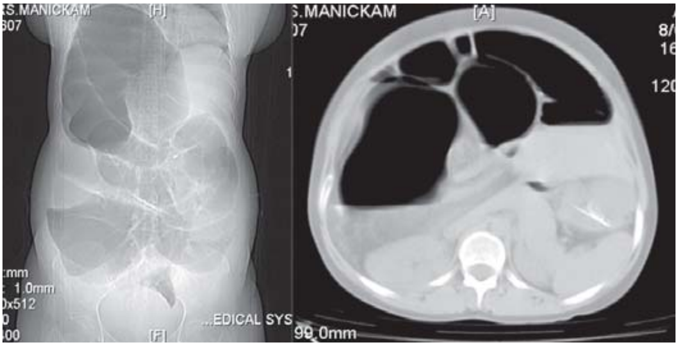

Digital scanogram showing dilated large bowel loop in the right upper quadrant. At surgery a transverse colon volvulus was seen.

PNEUMOPERITONEUM

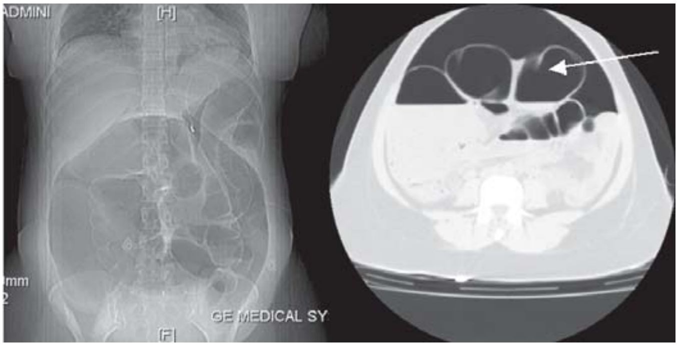

Digital scanogram showing centrally placed dilated bowel loops with increased lucency-the football sign of pneumoperitoneum. Axial NECT sections in lung window demonstrate gross pneumoperitoneum (arrow).

WHORL SIGN OF VOLVULUS

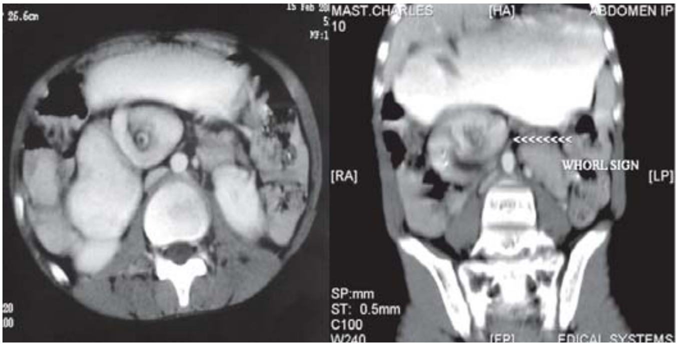

Axial CECT showing the classical whorl sign of midgut volvulus. This appearance is caused due to twisting of mesentery around the superior mesenteric artery axis.

NON-OCCLUSIVE MESENTERIC ISCHEMIA

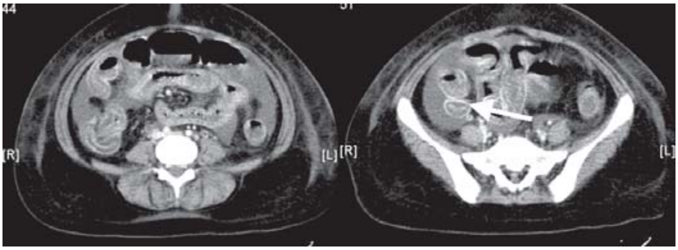

Axial CECT showing small bowel edema with intense serosal enhancement. Moderate peritoneal free fluid. Patient is a young female with SLE who has had multiple similar episodes in the past. The key to diagnosis is the clinical history and serosal enhancement.

EMPHYSEMATOUS PYELONEPHRITIS

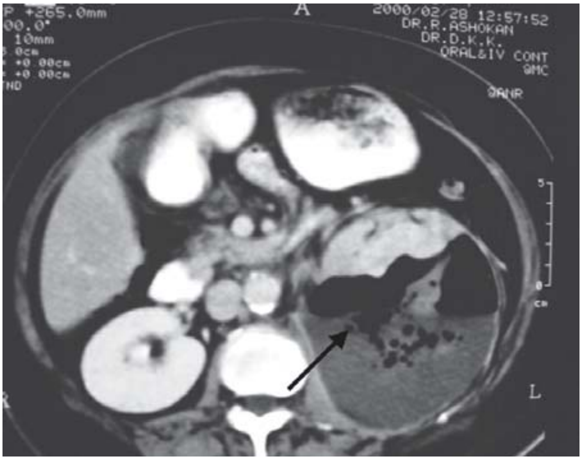

Axial CECT showing a large walled of lesion with air fluid level displacing the kidney anteriorly (arrow).

ACUTE PYELONEPHRITIS

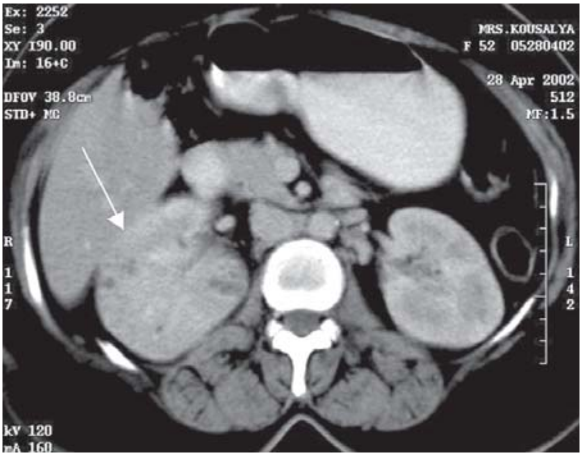

Axial CECT showing enlarged right kidney with altered attenuation showing punctuate hypodensities (arrow).

RENAL ABSCESS

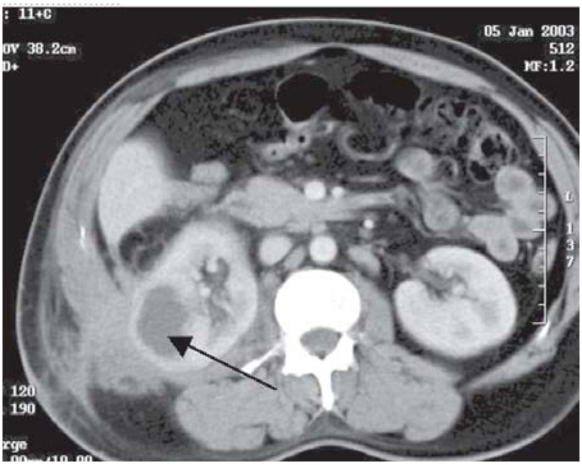

Axial CECT showing right interpolar low attenuation lesion suggestive of abscess involving the adjacent parietal wall (arrow).

ACALCULUS CHOLECYSTITIS

Axial CECT showing thickened gallbladder with no luminal calculus.

CALCULUS CHOLECYSTITIS

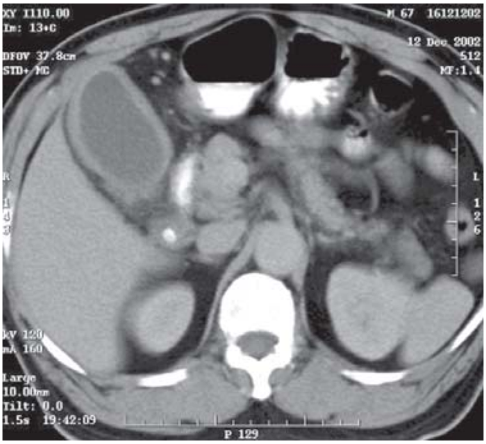

Axial CECT showing distended gallbladder with wall thickening, note the impacted calculi in the neck. No significant pericholecystic changes noted.

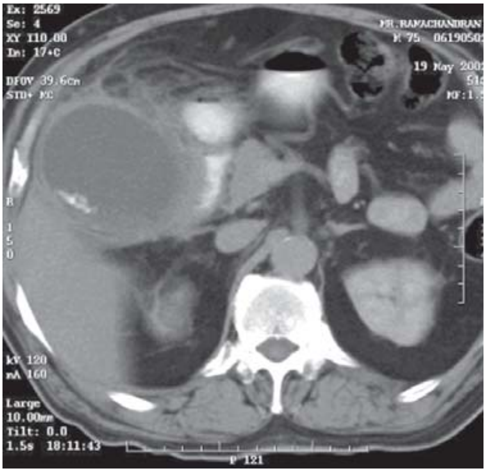

Axial CECT showing distended gallbladder with mural thickening and luminal calculi, note the extensive pericholecystic fat stranding (arrow).

CHOLEDOCHOLITHIASIS WITH LIVER ABSCESS

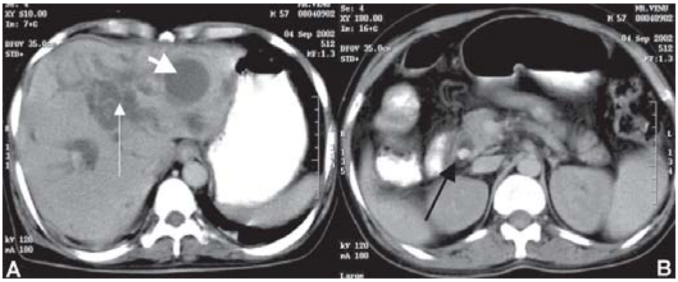

Axial CECT showing dilated intrahepatic biliary radicles (thin arrow Fig. A). Left lobe liver shows a hypodense lesion suggestive of abscess. Figure B shows the impacted terminal CBD calculus.

TARGET SIGN

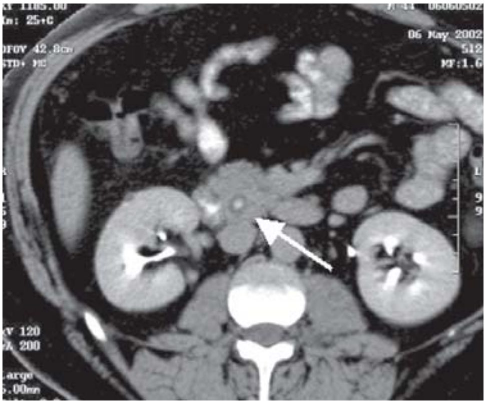

Axial CECT showing distal CBD calculus with a rim of bile causing the classical target sign of central high attenuation with peripheral lucent rim (arrow).

RECTUS SHEATH HEMATOMA

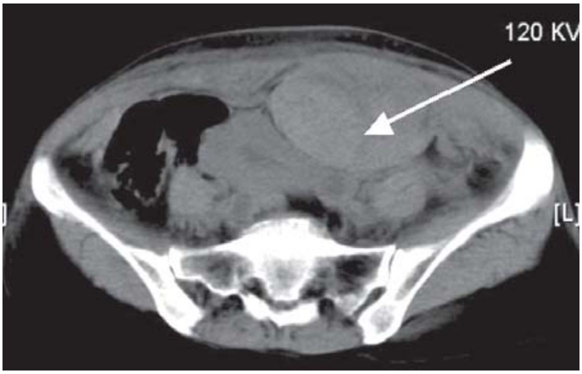

Axial CECT shows a left rectus sheath lenticular hyperdense lesion. Patient was an elderly lady who was receiving heparin for left MCA stroke.

RIGHT PARIETAL WALL ABSCESS

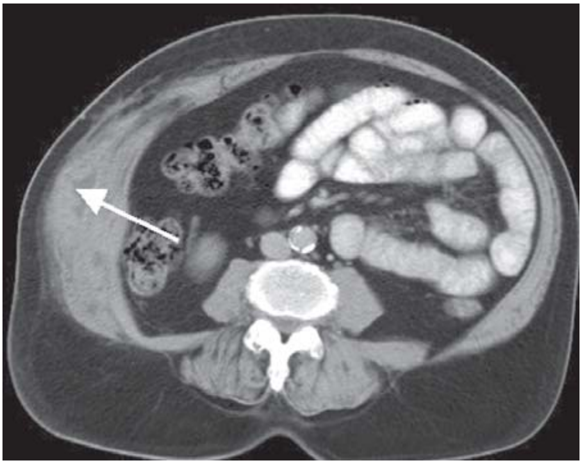

Axial CECT in a diabetic patient presenting with fever and pain in the right flank region with skin discoloration (arrow) shows right parietal wall phlegmonous changes with abscess formation.

PEUTZ-JEGHERS SYNDROME

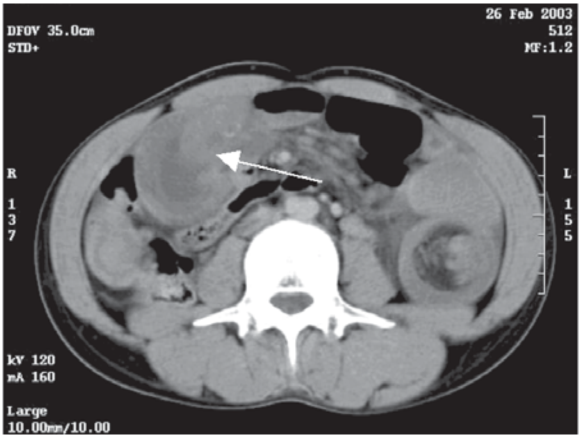

Axial CECT in a patient with recurrent abdominal pain reveals multiple intussusception with polyps (arrow).

TARGET SIGN

Bowel wall edema presents as circumferential thickening of the affected bowel loop demonstrating a hyperdense serosa, relatively hypoattenuating submucosa and mucosal hyperemia. This has been termed as the target appearance.

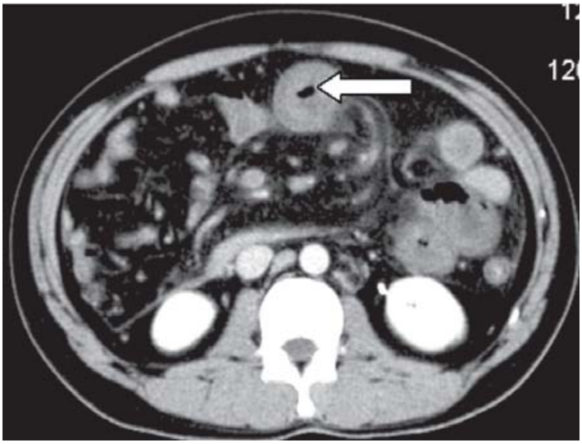

Axial CECT in a case with SMA thrombus showing the typical pattern of enhancemt in a ischemic bowel (target sign, arrow).

SMV THROMBOSIS

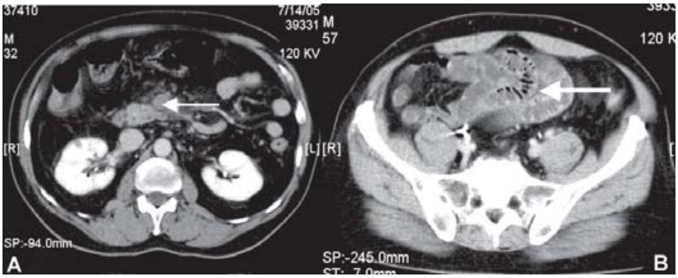

Axial CECT showing acute thrombus in the mesenteric vein (arrow in Fig. A). Note the dilated small bowel loops with enhancement and mural air pockets.

CLOSED LOOP SMALL-BOWEL OBSTRUCTION

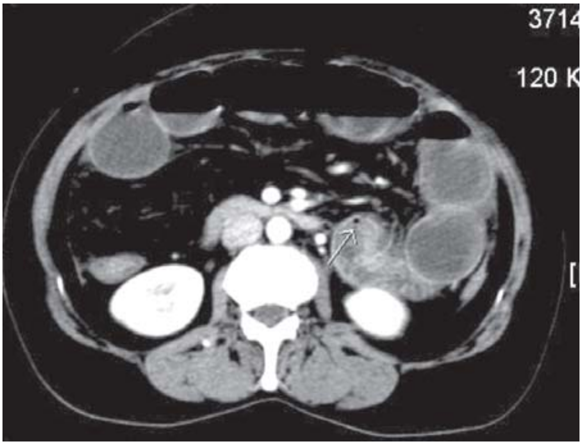

Axial CECT in a patient with small bowel obstruction showing proximal jejunal thickening with mural air pocket (segmental gangrene was found at surgery).

MESENTERIC VEIN GAS

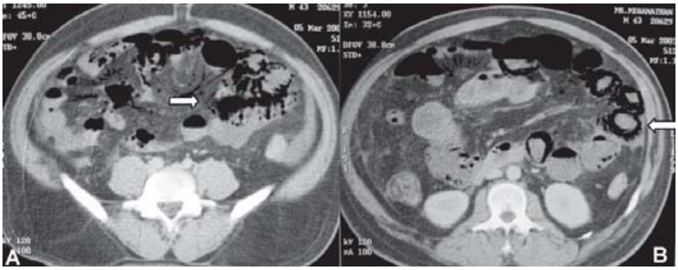

Axial CECT in a patient with SMA thrombus showing pneumotosis of the distal small bowels (arrow in Fig. B), note the air within the mesenteric vessels (arrow in Fig. A). Portomesenteric vein gas is most commonly caused by mesenteric ischemia but may have a variety of other causes. The primary factors that favor the development of this pathologic entity are intestinal wall alterations, bowel distention, and sepsis. Portomesenteric vein gas is idiopathic in approximately 15% of cases.

HENOCH-SCHÖNLEIN SYNDROME

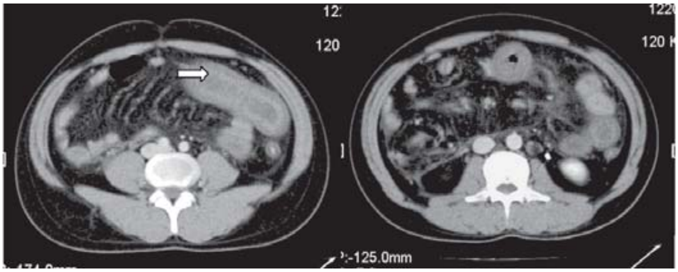

Axial CECT in a patient with known Henoch-Schönlein purpura presenting with abdominal pain showing thickening of distal jejunum showing mucosal enhancement (arrow).

When gastrointestinal symptoms predominate or precede the appearance of skin lesions, the syndrome may mimic a number of acute abdominal diseases, resulting in unnecessary laparotomies. Gastrointestinal hemorrhage is mostly confined to the mucosa and submucosa, and full-thickness necrosis and perforation of a bowel loop is rare. Therefore, most gastrointestinal manifestations are self-limited and without residua: only 3–5% of patients develop bowel infarct, perforation, or irreducible intussusception.

SMALL BOWEL OBSTRUCTION

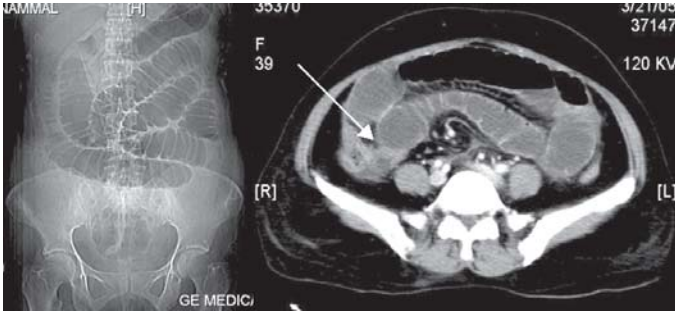

Digital scanogram showing grossly dilated small bowel loops (arrow), axial CECT showing a short segment ileal stricture (arrow) causing proximal bowel loop dilatation.

ARROW HEAD SIGN OF APPENDICITIS

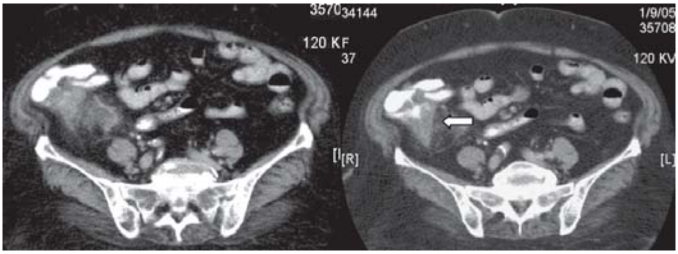

Axial CECT in a patient with right iliac fossa pain reveals the arrow head sign of appendicitis (arrow), note the periceacal inflammatory changes.

PSEUDOANEURYSM OF SMA

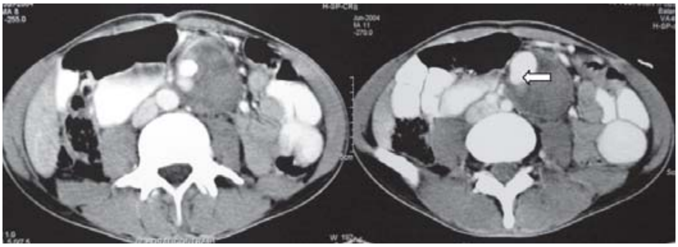

Axial CECT in a 46-year-old male with acute lower abdominal pain reveals a well marginated lesion showing a eccentric area of intense arterial enhancement – suggestive of pseudo-aneurysm arising from the branch of SMA.

ACUTE PANCREATITIS

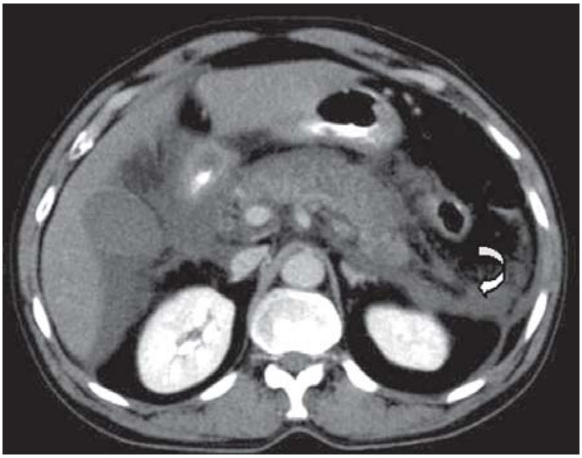

Axial CECT reveals hypodense edematous pancreatic parenchyma with rim of fluid, rim of fluid in the Morrison's pouch (arrow) with thickening of the left lateroconal and anterior gerotas fascia (curve arrow).

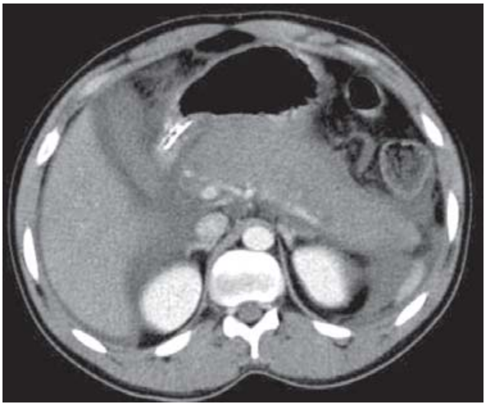

Axial CECT shows an enlarged edematous pancreas with peritoneal free fluid.

PANCREATIC ABSCESS

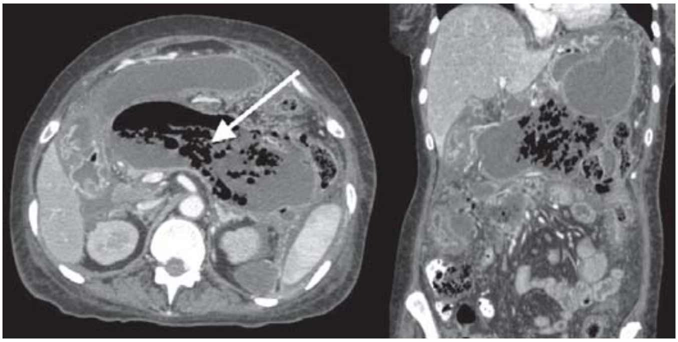

Axial CECT with coronal reformation studied shows multiple air airpockets with a large air fluid level in pancreas (arrow). There is total loss of normal pancreatic architecture. With extensive peritoneal inflammatory change.

LIVER ABSCESS

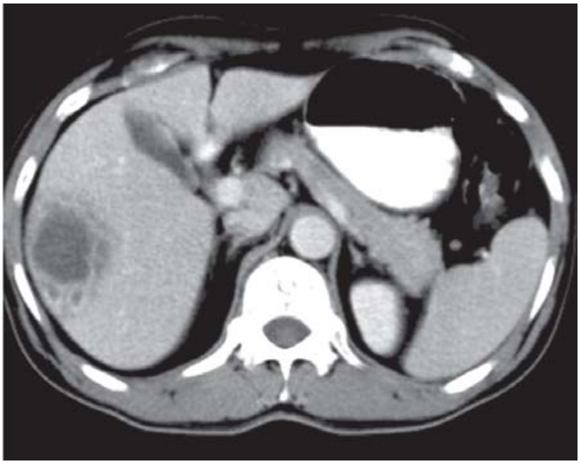

Axial CECT reveals a well marginated lesion in the right lobe inferior segment showing capsular enhancement with adjacent satellite nodules.

SMALL BOWEL PERFORATION

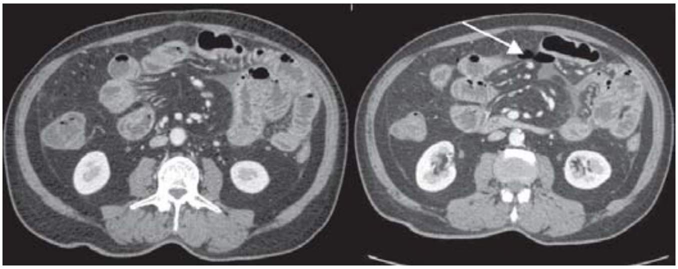

Axial CECT shows thickened small bowel loops showing mucosal enhancement with free air pockets in the adjacent periserosal mesentery.

WANDERING SPLEEN WITH INFARCTION

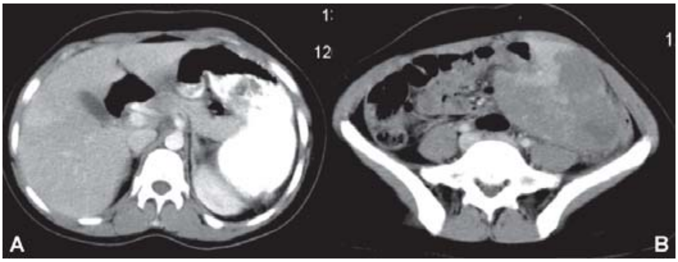

Axial CECT shows absence of spleen in its normal position, Figure B shows spleen in the left iliac fossa with multiple hypodense areas suggestive of infarcts.

SPLENIC INFARCTION

Axial CECT showing wedge-shaped hypodensity in the spleen suggestive of a spleen.

CRESCENT SIGN OF AORTIC ANEURYSM RUPTURE

A high-attenuation crescent sign was first described in 1988 by Pillari et al. This was the crescentic hyperattenuation area within the aortic wall or mural thrombus of AAA, which suggested penetration of blood into the mural thrombus. As the rupture progressed, the hemorrhage extended to the outer margin of the thrombus and was limited by the aortic wall.

SPONTANEOUS PSOAS BLEED

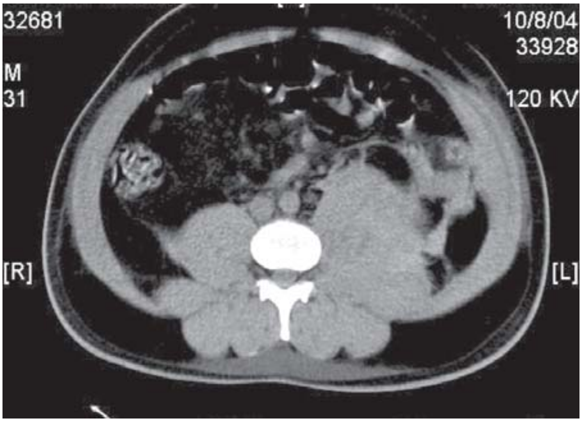

Axial CECT showing bulky left psoas with areas of high attenuation in a patient who had undergone thrombolysis for acute MI. Imaging features are suggestive of spontaneous psoas hematoma.

DUODENAL PERFORATION

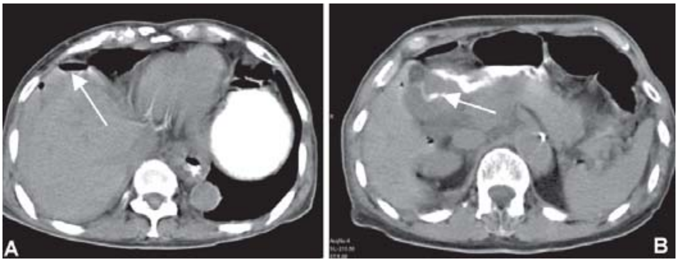

Axial CT with oral contrast shows peritoneal free fluid with perihepatic free air. Figure B shows thin track of contrast leaking from the duodenum (arrow).

RENAL CALCULI

Axial NECT with MIP CT nephrogram shows left distal renal calculus (arrow).

6. Traumatic Abdominal Emergencies

LIVER HEMATOMA

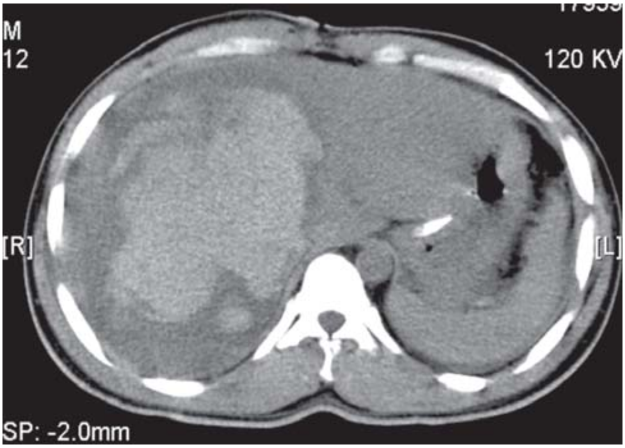

Axial NECT showing a large acute hematoma involving the right lobe of liver.

LACERATION

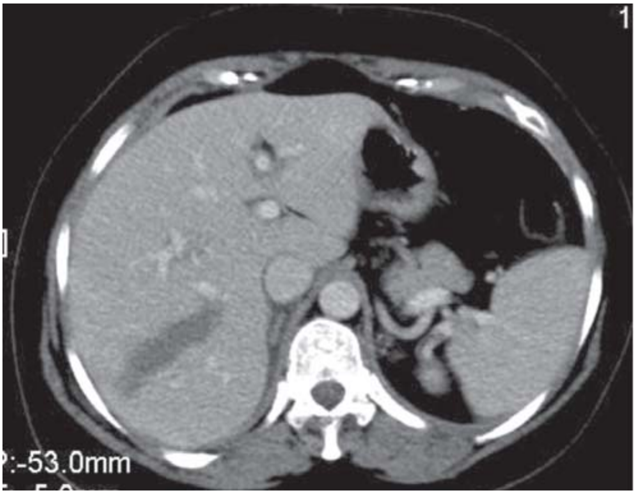

Axial CECT showing a linear hypodensity in the right lobe of liver suggestive of laceration.

SPLENIC LACERATION WITH CONTUSION

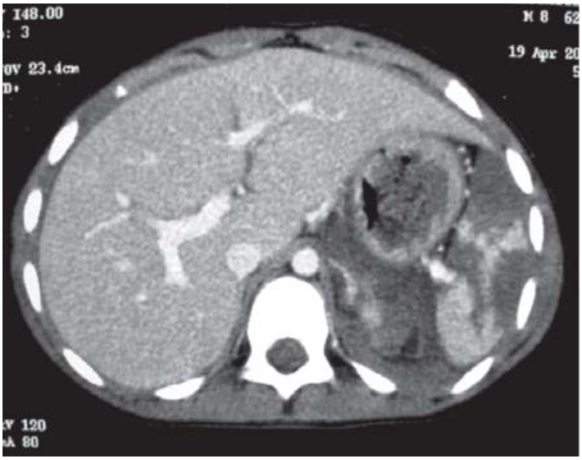

Axial CECT showing hypodense areas in the spleen at anterior and capsular margin suggestive of contusion. Linear hypodense areas in the splenic hilum is suggestive of laceration.

RENAL LACERATION

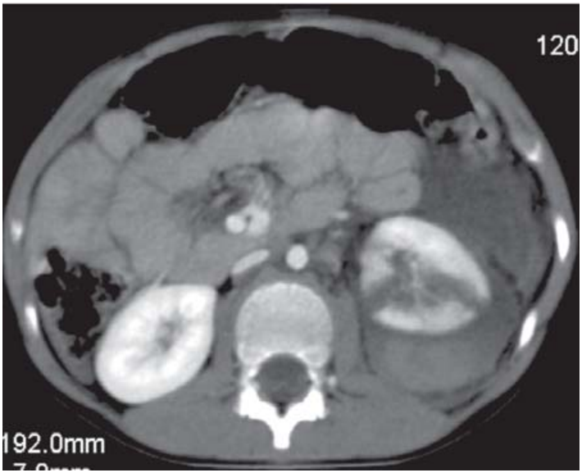

Axial CECT showing linear laceration with subcapsular hematoma involving the left kidney.

PANCREATIC LACERATION

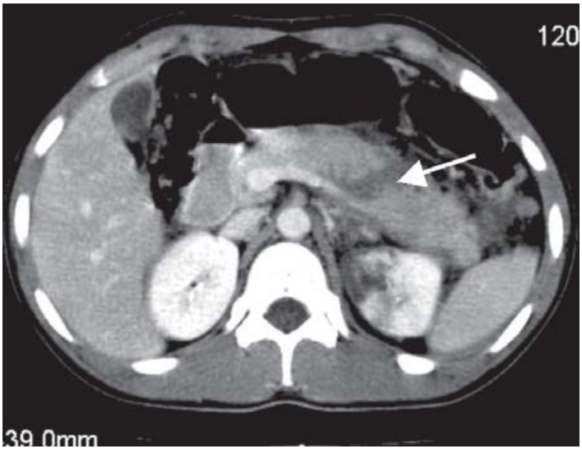

Axial CECT showing a linear hypodense area in the body of pancreas suggestive of contusion.

7. Musculoskeletal Trauma

INTRODUCTION

Standard Radiographs

- First examination obtained
- Can be done as portable exam
- Failure to diagnose unstable injury on arrival may lead to additional, permanent neurologic damage.
- Complementary to CT: some injuries subtle on axial images

The **advantages** of CT are:

1. CT is excellent for characterizing fractures and identifying osseous compromise of the vertebral canal because of the absence of superimposition from the transverse view. The higher contrast resolution of CT also provides improved visualization of subtle fractures.
2. CT provides patient comfort by being able to reconstruct images in the axial, sagittal, coronal, and oblique planes from one patient positioning.

The **limitations** of CT are:

1. Difficult to identify those fractures oriented in axial plane (e.g. Dens fractures).
2. Unable to show ligamentous injuries.

The **advantages** of MRI are:

1. Excellent soft tissue constrast, making it the study of choice for spinal cord survey, hematoma, and ligamentous injuries.
2. Provides good general overview because of its ability to show information in different planes (e.g. Sagittal, coronal, etc.).
3. Ability to demostrate vertebral arteries, which is useful in evaluating fractures involving the course of the vertebral arteries.
4. No ionizing radiation.

CERVICAL SPINE EVALUATION

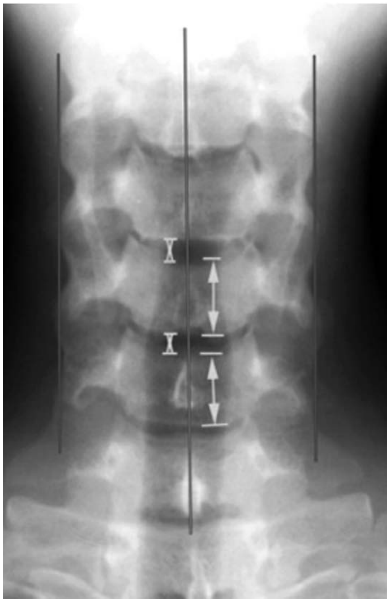

Alignment on the A-P view should be evaluated using the edges of the vertebral bodies and articular pillars. The height of the cervical vertebral bodies should be approximately equal on the AP view.

The height of each joint space should be roughly equal at all levels. Spinous process should be in midline and in good alignment. If one of the spinous process is displaced to one side, a facet dislocation should be suspected.

SOFT TISSUE SPACES

Prevertebral soft tissue swelling is important in trauma because it is usually due to hematoma formation secondary to occult fractures.

Nasopharyngeal space (C1) — 10 mm (adult)
Retropharyngeal space (C2-C4) — 5-7 mm
Retrotracheal space (C5-C7) — 14 mm (children), 22 mm (adults).

Soft tissue swelling in symptomatic patients should be considered an indication for further radiographic evaluation. If the space between the lower anterior border of C3 and the pharyngeal air shadow is > 7 mm, one should suspect retropharyngeal swelling (e.g. Hemorrhage). This is often a useful indirect sign of a C2 fracture. Space between lower cervical vertebrae and trachea should be < 1 vertebral body.

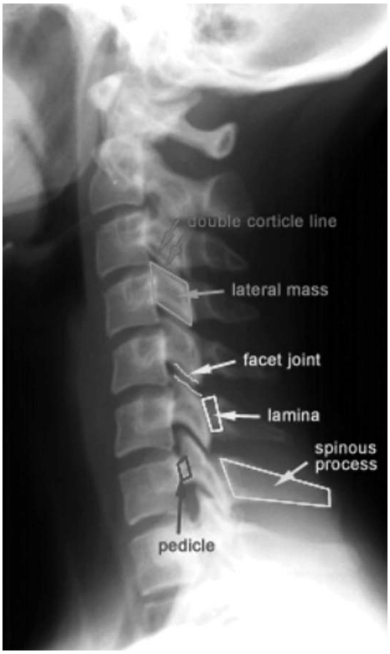

X-ray C spine lateral view with posterior elements highlighted.

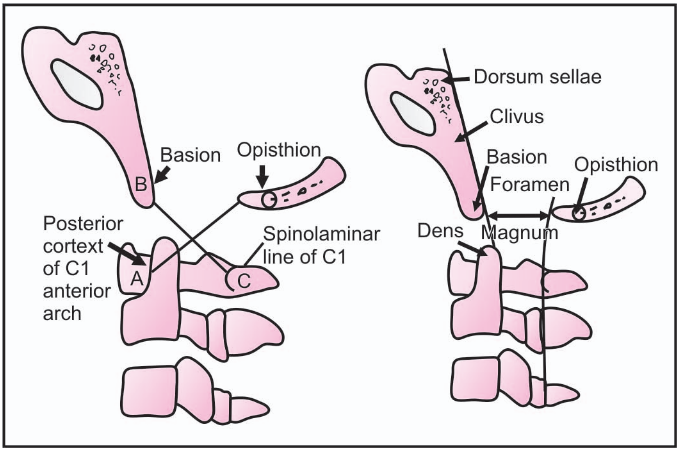

Schematic showing the various lines of the CVJ

The ratio of Basion - spinolaminar line of C1 to Opisthion-posterior cortex of C1 anterior arch normally ranges from 0.6 to 1.0, with the mean being 0.8. A ratio greater than 1.0 implies anterior cranio-cervical dislocation.

Assess four parallel lines. These are:

1. Anterior vertebral line (anterior margin of vertebral bodies)
2. Posterior vertebral line (posterior margin of vertebral bodies)

3. Spinolaminar line (posterior margin of spinal canal)
4. Posterior spinous line (tips of the spinous processes)

These lines should follow a slightly lordotic curve, smooth and without step-offs. Any malalignment should be considered evidence of ligamentous injury or occult fracture, and cervical spine immobilization should be maintained until a definitive diagnosis is made.

ODONTOID FRACTURE

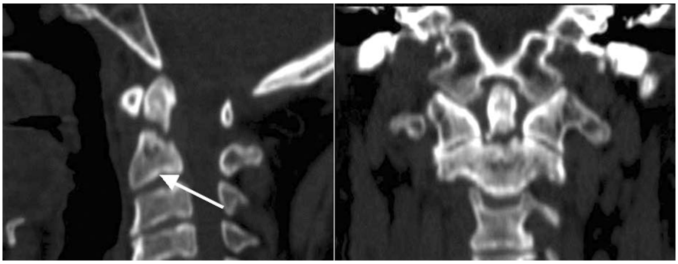

Sagittal and coronal MIP images showing fracture of the base of dens (arrow).

TRAUMATIC LISTHESIS

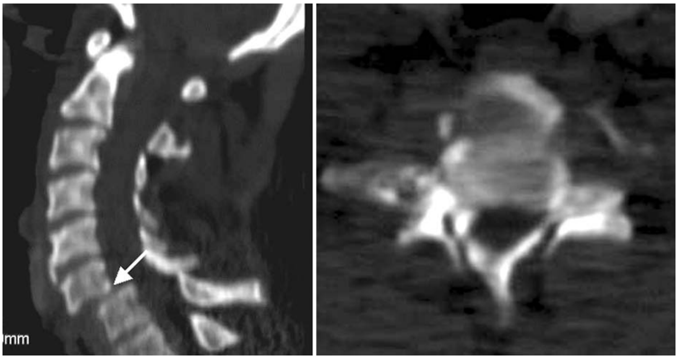

Sagittal reformation with axial CT showing anterior listhesis of C6/C7 vertebrae, note two endplates seen in the same axial slice.

C1 ARCH FRACTURE

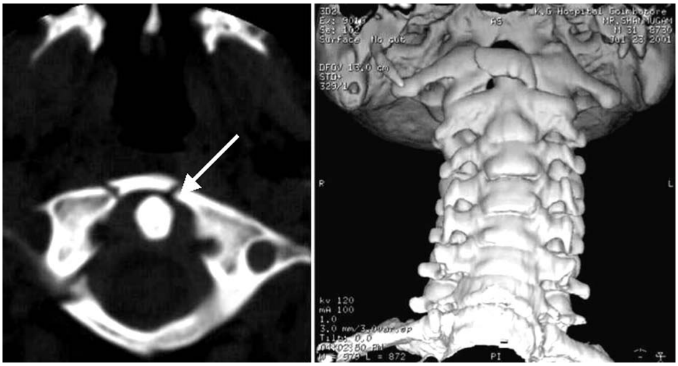

Axial CT with 3D SSD reformation studied shows fracture of the anterior arch of atlas involving the right lateral mass (arrow).

BURST FRACTURE

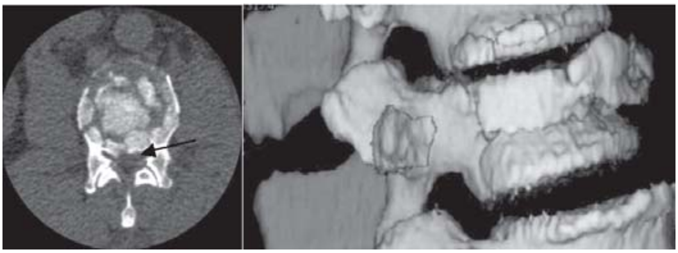

Axial CT with 3D SSD projection showing a burst fracture–note the fracture involving the posterior vertebral margin with epidural space involvement.

COLUMNAR STRUCTURE OF SPINE

- Spine structurally is described as tricolumnar
- Anterior, middle and posterior columns
- Each column has a component against compression force and another against tensile stress
- Bony and disk component resists compression force
- Ligamentous component resists tensile stress
- Anterior column
  - Bone: body centrum and disk
  - Lig: Anterior longitudinal ligament and anterior part of annulus fibrous
- Middle column
  - Bone: Posterior part of vertebral body and uncovertebral joints
  - Lig: Posterior longitudinal ligament and posterior part of annulus fibrous
- Posterior column
  - Bone: Lateral masses and facet joints
  - Lig: Capsule of facet joint and interspinous ligament

  Middle column by far the importance for the stability. If any two of the above three components fail, then spine can be unstable.

TRAUMATIC LISTHESIS WITH TRANSECTION OF CORD

Sagittal reformation with axial section showing D6/D7 complete listhesis with transection of cord, note two vertebral bodies at the same level.

MECHANISM OF SPINAL INJURY

Pathria and colleagues have classified the mechanisms of spinal injury as follows:

- Flexion
- Extension
- Rotary

- Compression
- Distraction
- Shear forces

These may produce damage by isolation or in combination.

Landmark MRI patterns described by Yamashita et al 1990, in patients scanned sequentially following injury:-

Type I- normal signal intensity on T1 and T2- with excellent prognosis and good neurological outcome.

Type II- normal signal on T1 and high signal on T2- this pattern has good neurological outcome if it resolves to type I, if type II pattern persists, it indicates no improvement.

Type III- low signal on T1 and high signal on T2- indicates myelomalacia

Type IV- atrophy

Type V- syrinx

Type III, IV and V all predict a poor outcome.

WHIP LASH INJURY

Sag T2 W and sag T1 W images —spondylotic changes are seen = disk bulges and osteophyte formation at C3-C4 and C4-C5 levels =in this patient with hyperextension injury has produced whip lash cord contusion. The PLL is intact. All is stretched by underlying hematoma. Hematoma is also seen in the dager space of the neck.

Prevertebral collections are best seen on T2 WI in sagittal plane.

EPIDURAL HEMATOMA

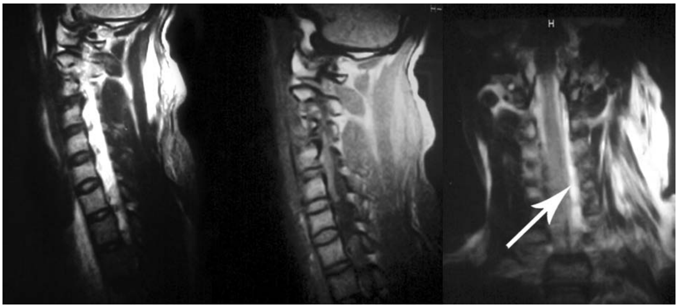

Sag T2W, sag T1W, coronal T2W

Epidural hematoma is seen in the left parasagittal imaging. The cord is displaced to the right and this is seen on the coronal images.

T1 WI are very important in detection of epidural bleeds as hyperintensity of the CSF and the hematoma may not be separately appreciated on T2WI.

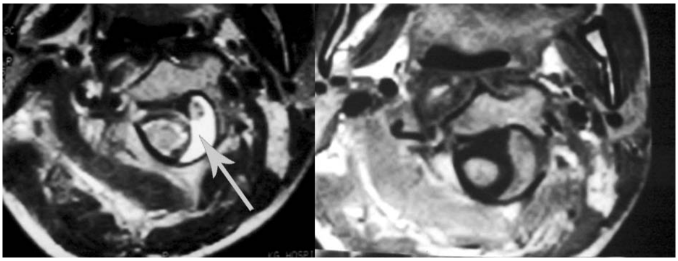

FSE T2 axial, T1W axial unusual collection of epidural hematoma in the contralateral side (left) with fracture through the right lateral mass of C2 vertebra. Nerve root encasement by the epidural hematoma is best made out on FSE T2 WI. Detection of the epidural hematoma is, however, easier on T1WI.

ODONTOID FRACTURE

T2W sagittal images of the C spine may help in detecting fractures of the odontoid which can be missed on conventional CT images as the plane of fracture may be parallel to the orientation of the slice direction.

FLEXION INJURY

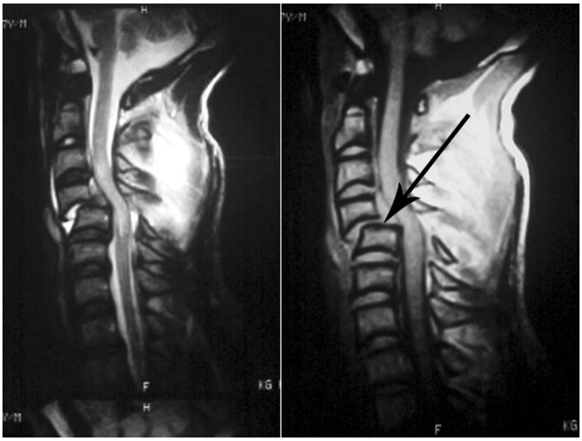

FSE T2W and T1W sag W disruption of all, PLL, flavum and interspinous ligaments are seen well on FSE T2 sagittal images. Traumatic discitis, prevertebral hematoma and cord contusion are also seen well on T2 WI. Characterization of the epidural mass as epidural hematoma is, however, made out best on T1 WI.

BRACHIAL PLEXUS INJURY

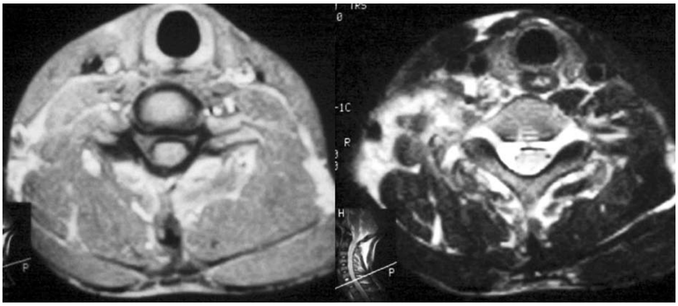

Axial T1 and T2 W images

This patient had epidural hematoma encasing the C6 roots on the Rt side at C5-C6 neural foramen. Paravertebral muscle contusion was also seen involving the scaleneus aterio, scaleneus medius muscles and the intervening brachial plexus roots, proximal trunks.

Epidural hematoma is seen well on T1 WI. Although muscle contusion can be suspected on T1 WI by the increase in muscle size and blurrin in outline it is made out well on T2 WI by the signal lengthening on FSE T2 WI.

FLEXION AND EXTENSION STUDIES

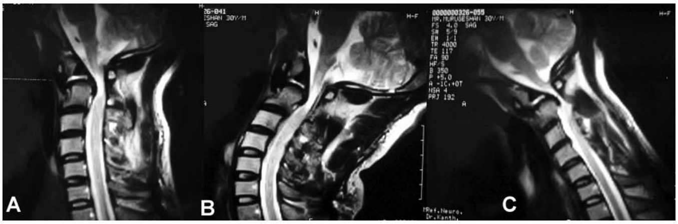

T2W sagittal weighted images showing odontoid fracture in neutral (Fig. A), extension (Fig. B) and flexion (Fig. C) positions. Extension studies show an intact PLL. There is increased indentation on the cord by C2 body on flexion.

FRACTURES OF HIP

3D SSD images showing fracture of the quadrilateral plate of the acetabulum.

COMPLEX ACETABULAR FRACTURES

Axial CT with 3D SSD image showing fractures involving the anterior, posterior acetabular columns and the quadrilateral plate.

DISLOCATION OF HIP

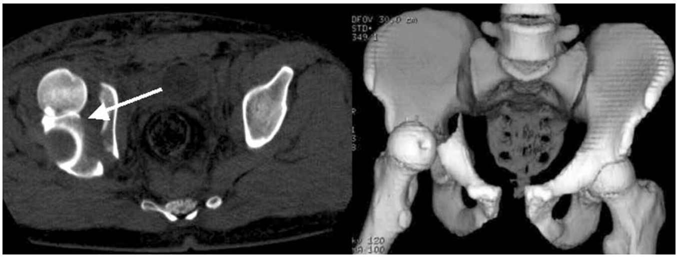

Axial CT with 3D SSD reformation shows fracture of the anterior acetabular column with anterior dislocation.

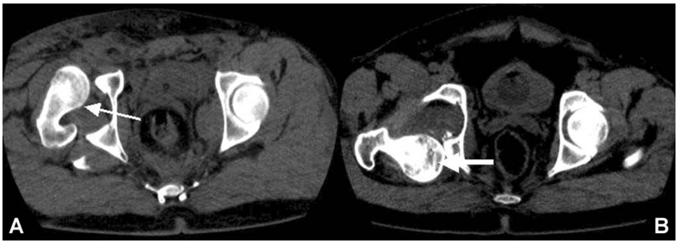

Axial sections showing anterior dislocation (Fig. A) and posterior dislocation (Fig. B) of the right hip.

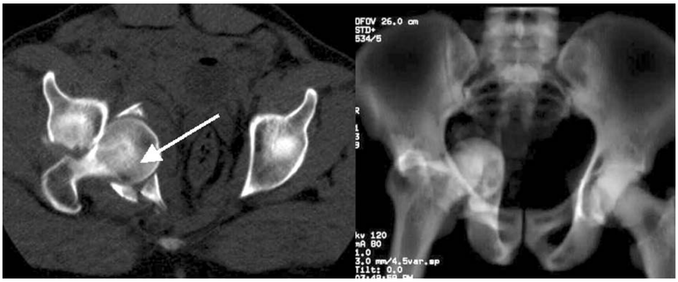

Axial CT with 3D Raysum projection showing central dislocation of the right hip (arrow).

TIBIAL PLATEAU FRACTURES

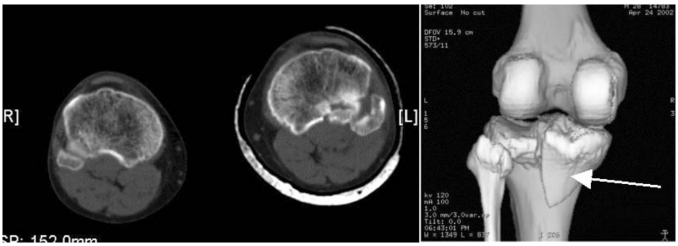

Axial CT with 3D SSD showing fracture of the left posterior tibial plateau with a separated fragments.

ARTICULAR FRACTURE OF DISTAL FEMUR

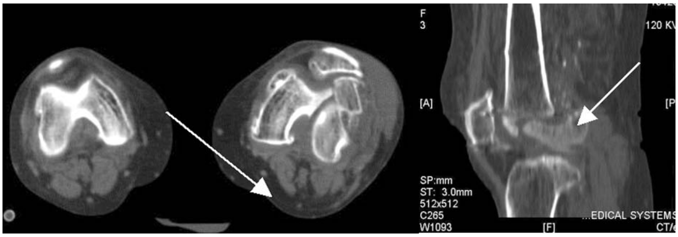

Axial CT with sagittal reformats through the knee showing a complex fracture involving the femural epiphysis with separation of the fractured fragment.

ARTICULAR FRACTURE WITH HEMARTHROSIS

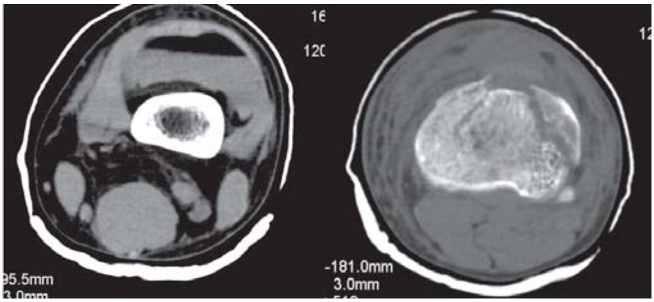

Axial CT sections showing fat fluid level in the supra-patellar bursa due to an anterior tibial plateau fracture.

PROXIMAL HUMERAL FRACTURES

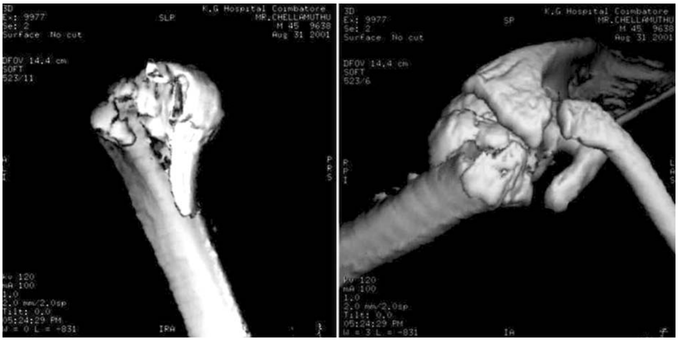

3D SSD images showing comminuted fracture of the right proximal humerus with a transarticular fractures.

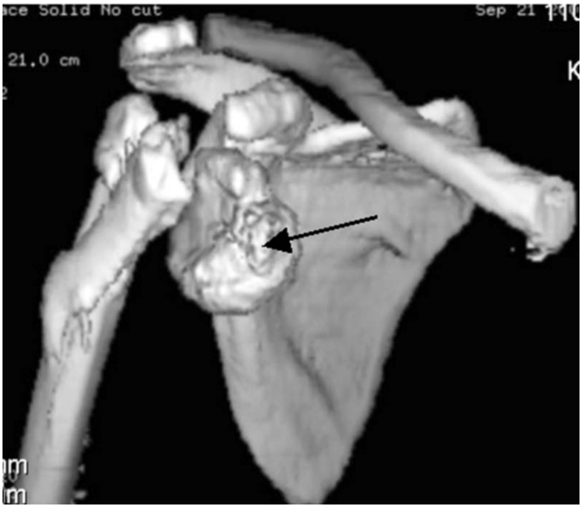

3D SSD image showing comminuted fracture of the right proximal humerus, with three part fracture separation.

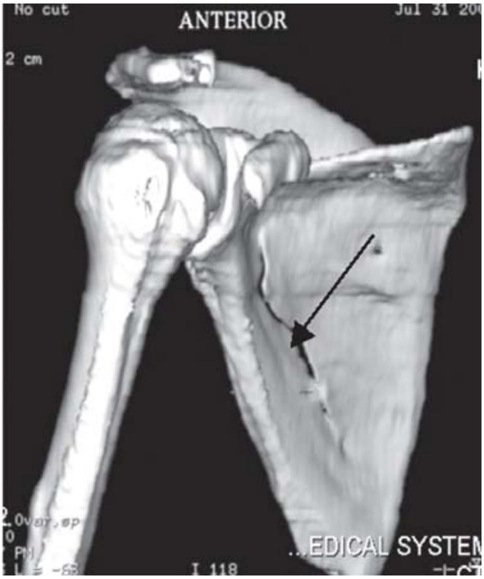

3D SSD reformats show a linear fracture of the scapular body.

FRACTURES AROUND THE ELBOW

3D MIP with SSD reformation shows fracture of the coronoid process of ulna.

3D VR images showing fracture of the capitulum of humerus.

FRACTURE AROUND THE WRIST

3D VR image showing fracture of the radial styloid process.

FRACTURE OF CARPAL BONES

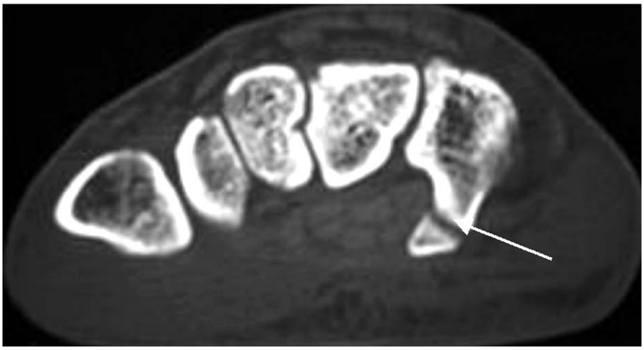

Axial high resolution images through the carpal bones show fracture of the hook of hamate.

SACROILIAC DIASTASIS

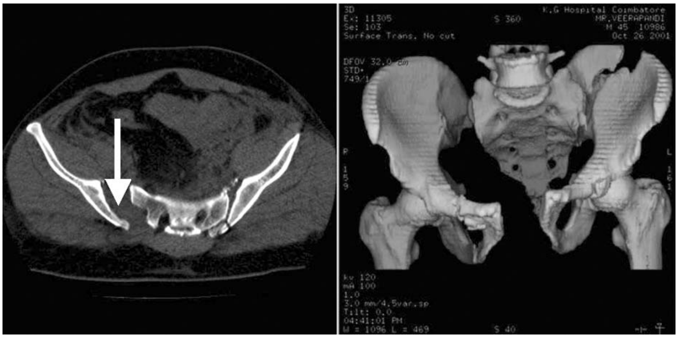

Axial CT with 3D SSD reformation shows diastasis of the right sacroiliac joint (arrow), also note the left iliac fracture involving the SI joint.

FACIAL FRACTURES

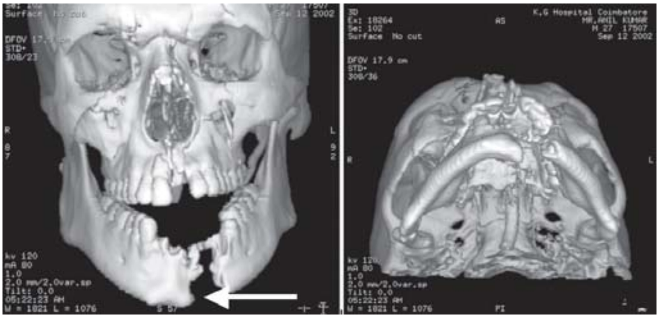

3D SSD reformation shows fracture of the mandibular symphysis with distraction.

MAXILLOFACIAL INJURIES

High-resolution CT imaging has replaced conventional radiography for the evaluation of facial trauma because of its widespread availability and fast imaging capability. CT can also be performed with less potentially hazardous positioning of injured patients.

Radiographic Signs of Facial Fractures

Direct Signs

- Nonanatomic linear lucencies
- Cortical defect or diastatic suture
- Bone fragments overlapping causing a "double-density"
- Asymmetry of face

Indirect Signs

- Soft tissue swelling
- Periorbital or intracranial air
- Fluid in a paranasal sinus.

The most common patterns of midfacial fractures are summarized in the table below.

Fracture Type		*Prevalence*
Zygomaticomaxillary complex (tripod fracture)		40 %
Le Fort	I	15 %
	II	10 %
	III	10 %
Zygomatic arch		10 %
Alveolar process of maxilla		5 %
Smash fractures		5 %
Other		5 %

Zygoma Fractures

Probably the most common facial fracture is the tripod or zygomaticomaxillary complex fracture, so called because it involves separation of all three major attachments of the zygoma to the rest of the face.

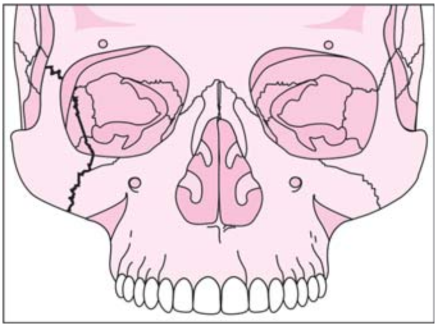

Frontal view of a zygomaticomaxillary complex fracture.

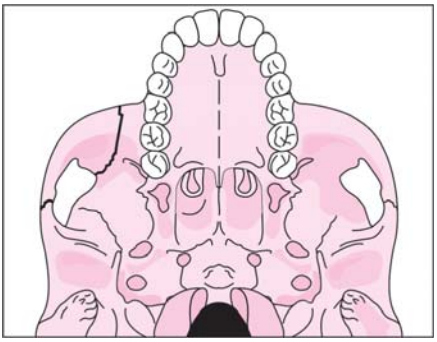

Submentovertex view of a zygomaticomaxillary complex fracture.

This fracture is usually due to a direct blow to the body of the zygoma. Occasionally, extraocular muscles may become entrapped in the zygomaticomaxillary component of the fracture complex. CT is extremely helpful in evaluating these fractures. It is therefore extremely important to obtain precise realignment of the fractured bone to prevent long-term visual changes.

Fractures may be isolated to the zygomatic arch. Clinically, these injuries are usually due to a blow from the side of the face. Patients with this injury often present with flatness of the lateral cheek area and inability to open their mouth, due to impingement of the zygomatic arch fragment upon the coronoid process of the mandible or the temporalis muscle.

Nasal-Orbital-Ethmoid Fractures

The nasal-orbital-ethmoid area is bordered by the orbital cavities laterally. Anteriorly, the space is demarcated by the frontal process of the maxilla, the nasal bones, and the frontal process of the frontal bone. Posteriorly, the boundary is the anterior aspect of the sphenoid bones and the roof is formed by the cribriform plate of the ethmoid bone. Injuries to this region of the facial skeleton generally occur from a direct frontal force. The diagnosis of fractures in this region is usually made by physical findings aided

by a CT scan. Routine films often fail to demonstrate the degree and location of the disruption. Special considerations of fractures in this region involve assessment of the lacrimal apparatus (tear duct system) and injury to the canthal ligaments. Disruption of the canthal ligaments can result in traumatic telecanthus (apparent widening of distance between the eyes).

BLOW OUT FRACTURES

Another common fracture is the orbital floor fracture, or "blowout" fracture. The usual mechanism is a blow to the eye, with the forces being transmitted by the soft tissues of the orbit downward to the thin floor of the orbit. The floor is usually the path of least resistance, and fractures downward into the maxillary sinus. On a Waters view, one may see a soft tissue mass on the superior margin of the maxillary sinus, representing the herniated periorbital tissues into the sinus. One may also see a "trapdoor" fragment of bone protruding down into the sinus, often hinged on the ethmoidal side. CT will, of course, show these fractures and soft tissue mass much better.

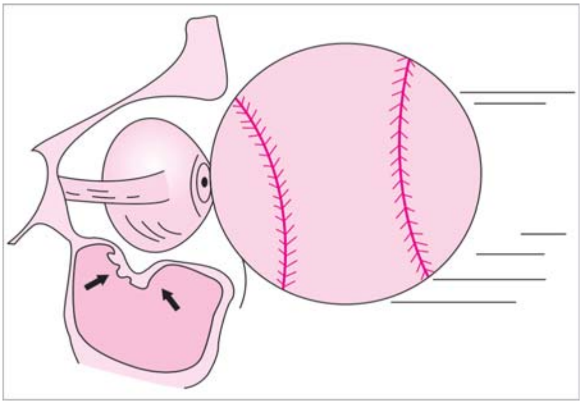

Blowout fracture" — the arrows point to the fracture fragments and periorbital tissue which have herniated into the maxillary sinus.

Le Fort Fractures

These are complex bilateral fractures associated with a large unstable fragment ("floating face") and invariably involve the pterygoid plates. Three main planes of "weakness" in the face, which correspond to where fractures often occur: the transmaxillary plane, the subzygomatic or pyramidal plane and a craniofacial plane.

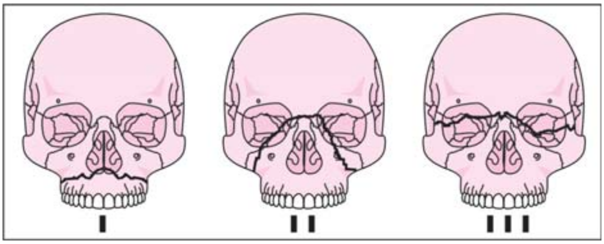

Frontal views of Le Fort complex fractures I - III.

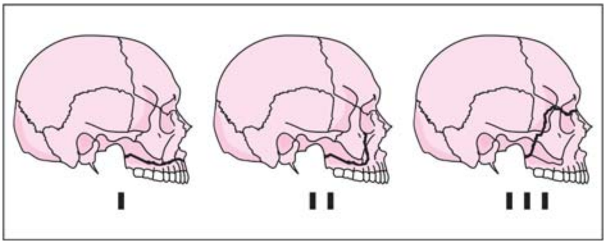

Lateral views of Le Fort complex fractures I - III.

The Le Fort I, or transmaxillary fracture runs between the maxillary floor and the orbital floor. It may involve the medial and lateral walls of the maxillary sinuses and invariably involves the pterygoid processes of the sphenoid. Clinically, the floating fragment will be the lower maxilla with the maxillary teeth.

The Le Fort II occurs along yet another weak zone in the face, and is sometimes called a pyramidal fracture because of its shape. A common mechanism is a downward blow to the nasal area.

The most severe of the classic Le Fort fracture complexes is the Le Fort III. I suppose that this is pretty obvious, given a three-part grading system. In this case, the large unstable (floating) fragment is virtually the entire face! Thus, this fracture is also referred to as craniofacial disassociation.

This is a very severe injury, and is often associated with significant injury to many of the soft tissue structures along the fracture lines. Generally, considerable force is necessary to produce this injury, and it is uncommon as an isolated injury. It may also occur in association with severe skull and brain injuries.

With the exception of the Le Fort I injury, "pure" Le Fort injuries are not commonly seen. More commonly seen are variants of the Le Fort classification. One of the most common of these is the Le Fort II - tripod fracture complex. This complex is usually due to the large forces encountered in a motor vehicle accident.

Besides the classic Le Fort patterns and the mixed Le Fort variants, there is another common pattern which is called, for obvious reasons, a "smash" fracture. In these injuries, severe comminution of the face is present, and underlying skull injury is likely. These patients are often in unstable condition with associated axial and appendicular skeletal injuries as well. This category includes several varieties of otherwise unclassifiable fractures, which are named for the portion of the face primarily involved.

Evaluation and management strategies for specific maxillofacial injuries		
Suspected injury	*Physical exam*	*Radiology*
Frontal bone fracture	Palpate periorbital rim Test for forehead anesthesia EOM testing	Skull film/Caldwell view CT frontal bone/sinus
Blowout fracture	Test for infraorbital anesthesia EOM testing Subcutaneous air Visual testing	Water's view CT orbits, especially coronal/sagittal views
Nasal fracture	Septal hematoma Cosmetic deformity	None necessary in adults, individualize in children
Tripod fracture	Lateral subconjunctival hemorrhage Drooping lateral canthus Test for infraorbital anesthesia Examine for open bite	CT face/orbits
Zygomatic arch fracture	Intraoral palpation Worm's eye/Bird's eye views	Submental vertex view
Le Fort fracture	Mid-face mobility Facial lengthening Examine for open bite	CT face
Mandibular fracture	ROM jaw Spatula test Dental exam Lower lip anesthesia	Panorex Towne's Lateral oblique mandible

Orbital Fractures

Orbital fractures may be isolated or occur as a component of more complex mid-face fractures, including the tripod fracture, the Le Fort II and the Le Fort III fractures. Isolated orbital fractures may involve one or more of the following: floor, the lamina papyracea, roof, or lateral wall. Orbital floor fracture (inferior blow out) results from a direct blow to the orbit by an object that is too large to enter the orbit. The force of the blow is absorbed by the orbital rim and is transmitted to the thinner orbital floor, which usually fractures in the middle third near the infraorbital canal.

Herniation of orbital fat, inferior rectus muscle, or the inferior oblique muscle can occur with muscle entrapment, resulting in diplopia.

Fracture of the lamina papyracea (medial blow out) may occur either as an isolated fracture or in conjunction with an orbital floor fracture. Orbital emphysema, resulting from the ethmoid sinus fracture occurs commonly in patients with medial blowout. Herniation of orbital fat and entrapment of medial rectus muscle may occur.

The blow-in fractures involve the orbital roof with inferior displacement of fracture fragments into the soft tissues of the orbit. In more than half of such cases, it is associated with frontal sinus or skull fractures.

Musculoskeletal Trauma

Ocular trauma classification
Closed-globe injury The eyewall does not have a full-thickness wound.
Open-globe injury The eyewall has a full-thickness wound—a through-and-through injury.
Rupture Full-thickness wound caused by blunt impact and an inside-out mechanism.
Laceration Full-thickness wound by sharp object.
Penetrating injury Single laceration, usually by a sharp object.
Perforating injury Two full-thickness lacerations (entrance + exit) usually caused by sharp object or missile

Approach to Orthopedic Radiograph

Misinterpretation of radiographic studies is a common source of medical error in both the inpatient and outpatient arenas. Of particular concern is the significant number of misinterpretations of plain radiographs.

The prevalence of this patient safety issue may result from the large volume of patients receiving these radiologic

tests, which are often done outside normal working hours when radiologists are not available to provide an initial interpretation.

Plain radiographs remain pivotal in the initial assessment of patients with a suspected fracture or dislocation. The radiographic approach should be tailored to the patient's history and physical examination. The possibility that an unusual or unexpected finding may represent a normal physical variant should always be considered.

Identify the radiographic features of fractures and dislocations.
Identify associated occult injuries

ABC SYSTEM OF ANALYSIS:
A-ADEQUACY, ALIGNMENT
B-BONES
C-CARTILAGE
SOFT TISSUE

Musculoskeletal Trauma

Commonly-missed Orthopedic Injuries

Body part	*Dislocation*	*Occult fracture*	*There is more than one injury present*
Wrist	Scapholunate dissociation Perilunate dislocation Lunate dislocation	Scaphoid Triquetrum	Galeazzi fracture-dislocation Distal radius fracture + carpal injury
Elbow	Radial head dislocation	Radial head	Monteggia fracture-dislocation
Pelvis/ Hip	Hip dislocation	Femoral neck Sacrum Acetabulum	Pelvic ring disruption
Knee	Knee dislocation	Tibial plateau Segond patella	Maisonneuve fracture
Foot	Lisfranc injury	Calcaneus Talus	Calcaneus + Thoracolumbar fracture

WRIST

The complex anatomy of the wrist lends itself to a myriad of injury patterns. The normal radiographic anatomy of the wrist can be seen in Figures 1 and 2. In a normal PA view, visualization of three smooth arcs is essential. These arcs are drawn along (1) the proximal aspect of the proximal row of carpal bones, (2) the distal aspect of the proximal row of carpal bones, and (3) the proximal aspect of the distal row of carpal bones. Further, the intercarpal distance should be less than 3 mm. Disruption of any of these arcs or an increase in the normal intercarpal distance suggests a fracture or dislocation.

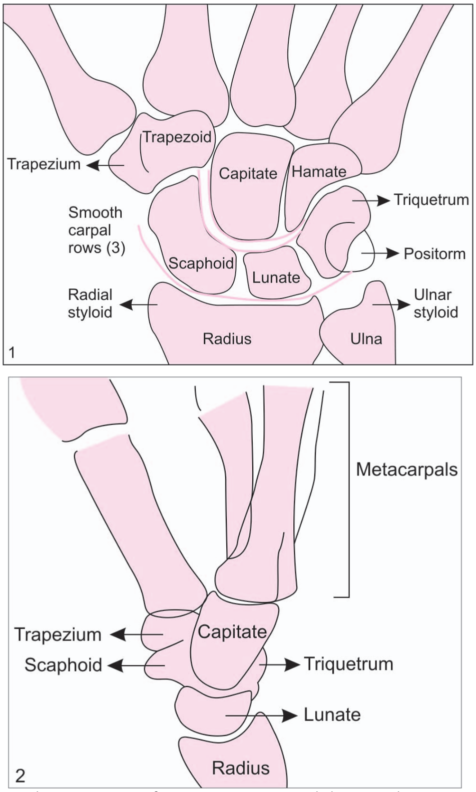

Schematic of wrist PA and lateral view showing the normal alignment.

ELBOW

Elbow radiographs are notoriously poor in directly detecting fractures. Indirect signs such as fat pads and bony misalignments are often the only suggestions of an injury. These fat pads can become displaced by an intra-articular effusion such as a hemarthrosis. This anterior fat pad is considered abnormal, however, when it becomes displaced and elevated (called a “sail sign”).

In contrast, the presence of any posterior fat pad, regardless of size and displacement, is pathological.

Bony alignment: The first alignment is the radio-capitellate line. On both the AP and lateral views, a longitudinal line drawn through the midshaft of the radius should bisect the capitellum. Any misalignment suggests a radial head dislocation.

The second line is the anterior humeral line. On a lateral view, a longitudinal line drawn along the anterior aspect of the humerus should bisect the capitellum.

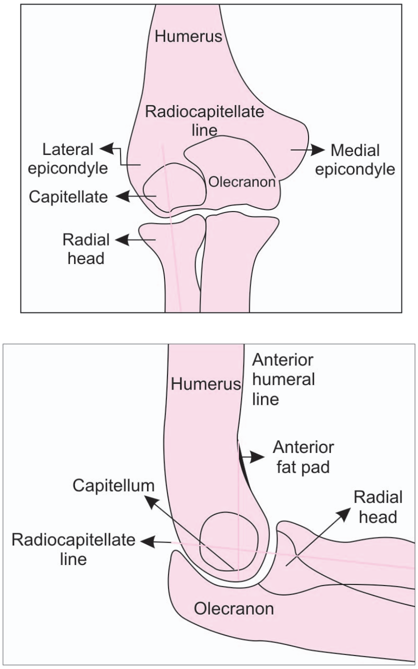

Schematic showing normal AP and lateral view showing the normal alignment.

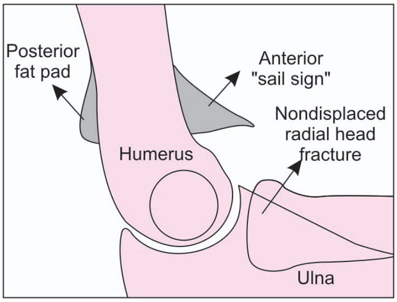

Schematic showing the indirect signs
of occult elbow fractures.

PELVIS AND HIP

The pelvis and hip are radiographically complex structures, and fractures in these areas comprise a substantial portion of missed fractures. Overlapping bones and the oblique orientation of many structures on the AP view are often the cause of radiographic misinterpretations.

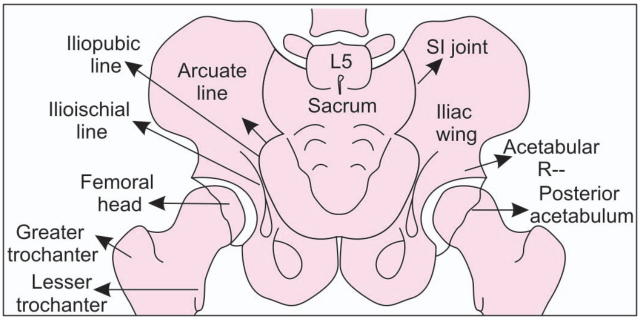

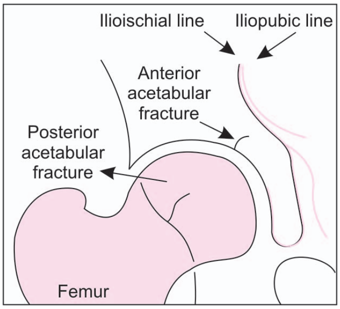

Schematic showing the normal alignment of hip in AP view.

There are three extremely important "O"ccult fractures of the pelvis and hip which require careful scrutiny. The first is a femoral neck fracture - the most commonly missed hip fracture.

The second "O"ccult fracture is of the sacrum.

And the third "O"ccult fracture involves the acetabulum, the pelvic articulation site for the femoral head. The acetabulum can be divided into anterior and posterior columns.

KNEE

Plain radiographs of the knee usually include an AP and lateral view. With this two-view imaging protocol, the sensitivity of detecting knee fractures is only 79 percent. The addition of two oblique views for a four-view imaging protocol increases this sensitivity to 85 percent. To reduce the number of overlooked knee fractures, consider obtaining oblique plain radiographs and possibly even CT imaging for high-risk patients.

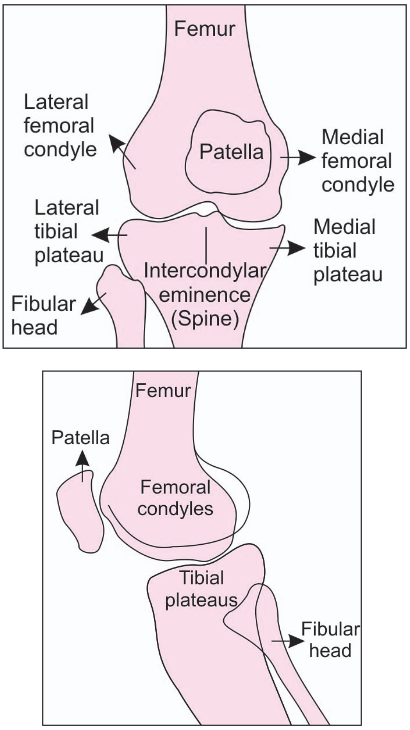

Schematic showing normal alignment around the knee.

There are three high-risk, "O"ccult fractures of the knee. The first is a tibial plateau fracture, which alone accounts for one-third of all knee fractures.

The second "O"ccult knee fracture is a Segond fracture—a proximal lateral tibial avulsion fracture. The fractured piece was the insertion site of the lateral capsular ligament. Although the fracture piece appears clinically insignificant, be wary that Segond fractures have a significant concurrent risk for anterior cruciate ligament (ACL) tears.

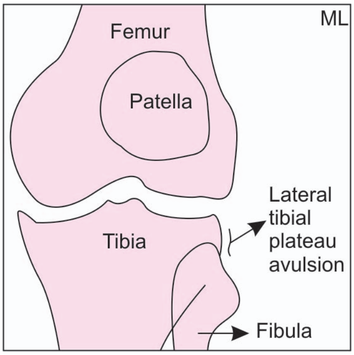
Femur
ML
Patella
Lateral
tibial
plateau
avulsion
Tibia
Fibula

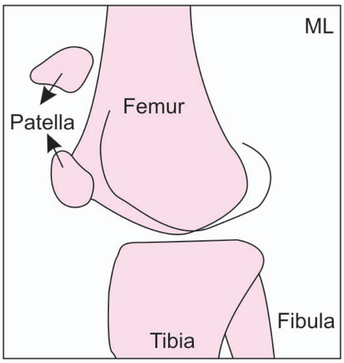
ML
Patella
Femur
Fibula
Tibia

Third "O"ccult fracture is a patella fracture, which comprises 40 percent of all knee fractures. It is usually the result of direct blunt trauma to the patella. Because of the overlapping femoral condyles, the AP view is poor in detecting patellar fractures.

The primary "H"alf pathology for the knee is a Maisonneuve fracture. In this injury, a fracture of the proximal fibula is associated with a fracture of the medial malleolus or deltoid ligament of the ankle. Often the ankle mortise is widened, and the tibiofibular syndesmosis is disrupted.

FOOT

Adequate imaging of the foot includes an AP, oblique, and lateral view. In addition to looking for cortical disruptions, examining alignments and measuring angles are essential in detecting subtle pathology. On the AP view, the lateral aspects of the first metatarsal and the first cuneiform should align, as should the medial aspects of the second metatarsal and the second cuneiform. On the oblique view, the medial aspects of the third metatarsal and third cuneiform should align. On the lateral view, Bohler's angle is generated by a line bordering the superior aspect of the posterior calcaneal tuberosity intersecting a line connecting the superior talar articular surface with the superior aspect of the anterior calcaneal process.

This angle measures 20 to 40 degrees normally.

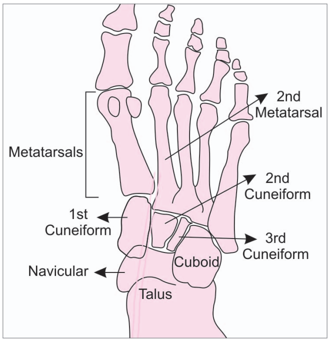

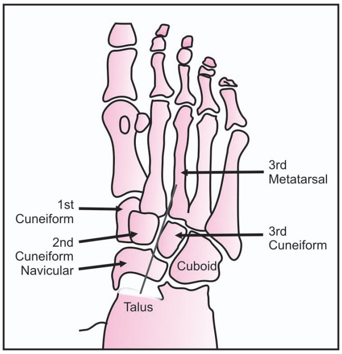

Schematic showing normal alignment of the tarsal and metatarsal bones.

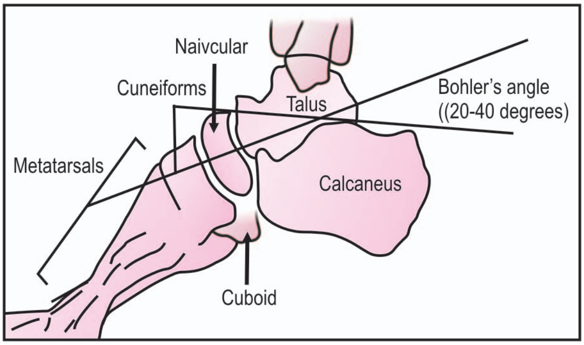

Schematic showing the normal Bohler's angle.

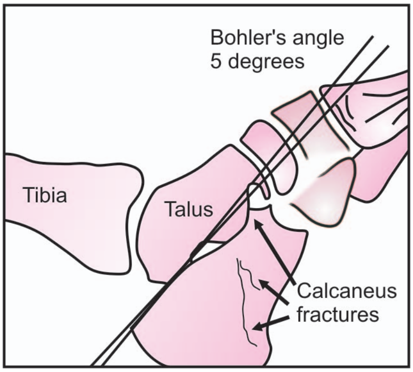

Two "O"ccult fractures of the foot include the calcaneus and talus fractures. Commonly this fracture occurs after a patient falls from a height onto his or her heel. Radiographic findings include a cortical break, and a Bohler's angle of less than 20 degrees suggests an impaction fracture. Calcaneal fractures frequently require CT imaging to further assess the severity of bony fragmentation.

The second "O"ccult fracture, a talus fracture, ranks as the second most commonly fractured tarsal bone. Anatomically, the talar neck is the site of the majority of these fractures.

8. CT Angiography

CT PERFUSION IN ISCHEMIC STROKE

Perfusion CT

Brain Perfusion—Perfusion of normal brain tissue is maintained within a narrow range by autoregulation of the cerebral vasculature. Normal blood flow in human gray matter is about 50-60 mL/100 g/min. In cases of occlusion of a major artery like the MCA, the survival of brain tissue depends on the minimum necessary collateral supply from leptomeningeal anastomoses.

1. At a cerebral blood flow (CBF) of 35 mL/100 g/min or less (i.e., approximately 50-60% of normal values), protein synthesis within neurons ceases completely. In this oligemic stage, tissue can survive as long as CBF is not further reduced.
2. At a CBF of 20 mL/100 g/min or less (i.e., approximately 30-40% of normal values), synaptic transmission between neurons is disturbed, leading to loss of function of still viable neurons. Ischemic brain tissue that is

"living" under these conditions adjacent to already irreversibly damaged tissue is defined as tissue at risk.

3. At a CBF of 10 mL/100 g/min or less (i.e., 20% of normal values), irreversible cell death occurs. Reperfusion of tissue at risk within a therapeutic window of 3 hours or even more can lead to complete regeneration of neuronal function.

Typical parameters used to describe cerebral perfusion include:

1. Mean transit time (MTT), that is, the time between arterial inflow and venous outflow.
2. Time to peak (TTP), which is often calculated in perfusion CT studies and represents the time from the beginning of contrast material injection to maximum (peak) enhancement within an intracerebral region of interest (ROI).
3. Cerebral blood volume (CBV), that is, the volume of blood per unit of brain mass. Normal CBV is about 4-5 mL/100 g. Under normal conditions, the relationship between CBF and CBV is expressed by the equation $CBF \_ MTT \_ CBV$.

When the capillary bed dilates in the early stage of ischemia, CBV will remain unchanged or even increase despite a decrease in CBF. When the mechanisms of autoregulation can no longer compensate for a further

reduction in CBF, CBV will also decrease. Therefore, simultaneous analysis of CBF and CBV as calculated from perfusion CT data is necessary to predict the volume of irreversibly damaged brain tissue and thus develop a prognosis for ischemic stroke.

Algorithm for fast interpretation of perfusion CT data within 3 hours of stroke onset

	Perfusion CT finding		
Pathologic condition	*TTP*	*CBF*	*CBV*
None	Normal	Normal	Normal
Arterial stenosis or occlusion with excellent compensation	Prolonged	Normal	Normal
Oligemic tissue that will probably survive	Prolonged	Moderately reduced (> 60%)	Normal or slightly reduced (>80%)
Tissue at risk	Prolonged	Markedly reduced (> 30%)	Moderately reduced (>60%)
Tissue that is probably irreversibly damaged	Strong prolongation or not measurable	Severely reduced (< 30%)	Severely reduced (< 40%)

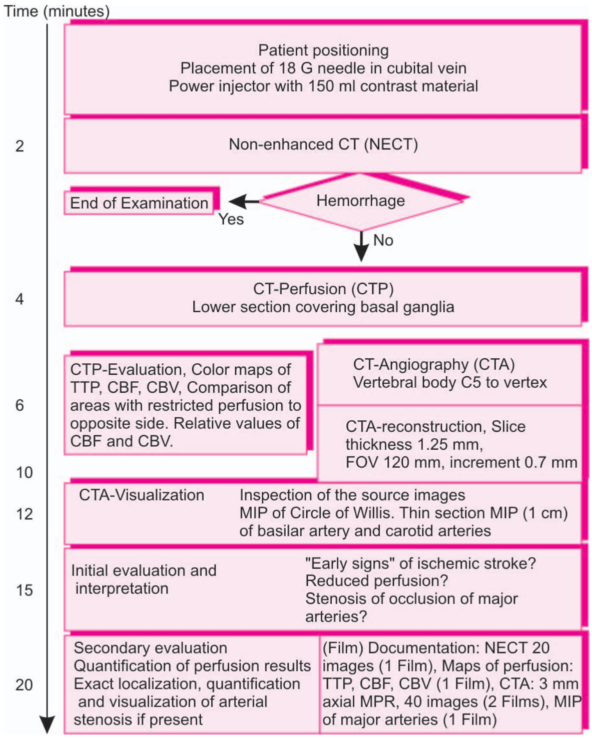

Protocol for evaluating stroke patients with multisection CT and the average time needed to complete each step. *CBF* – cerebral blood flow, *CBV* – cerebral blood volume, *MIP* – maximum intensity projection, *MPR* – multiplanar reformatting, *TTP* – time to peak.

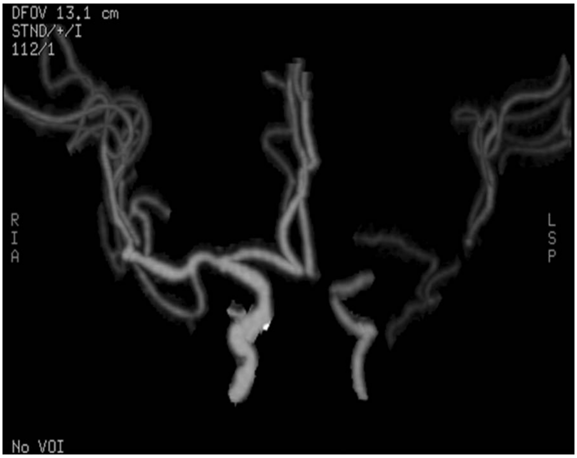

3D MIP angiogram showing occlusion of left MCA M1 and M2 segments.

A

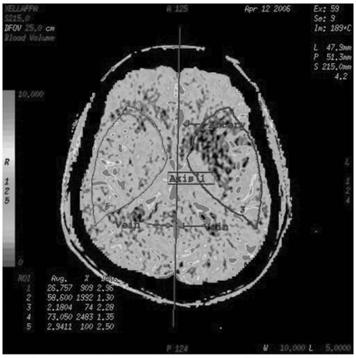

Blood volume

B

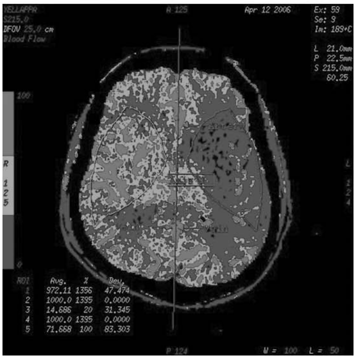

Blood flow

C

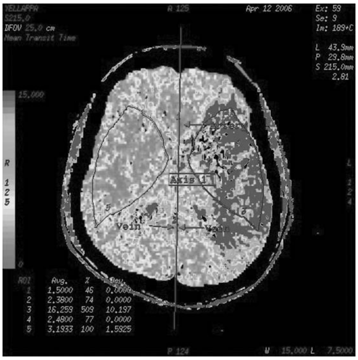

Mean transit time

CT perfusion maps
(For colour version see Figs 2A to C, Plate 3)

CT ANGIOGRAM OF NECK VESSELS

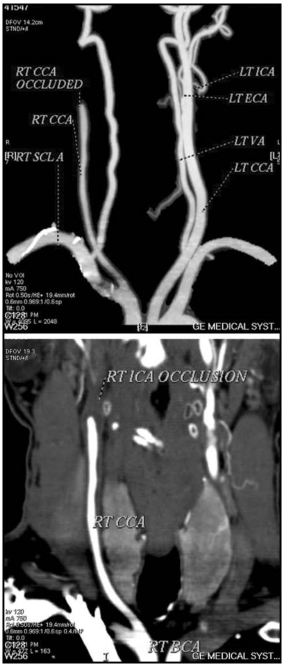

3D MIP and curved MPR images showing occlusion of right ICA from the origin *(For colour version see Fig. 3, Plate 4).*

CT ANGIOGRAM OF CIRCLE OF WILLIS

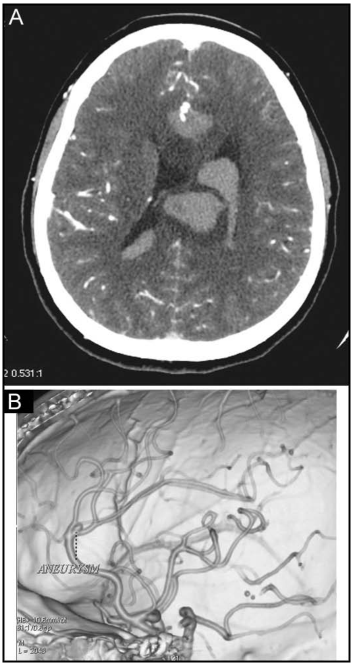

A

B

(A) Axial CT showing pericallosal hematoma, (B) Volume rendered image showing the acomm aneurysm *(For colour version see Figs 4A and B, Plate 5).*

Axial CT and VR image of circle of Willis showing occluded left vertebral artery *(For colour version see Fig. 5, Plate 6).*

CT AORTOGRAM

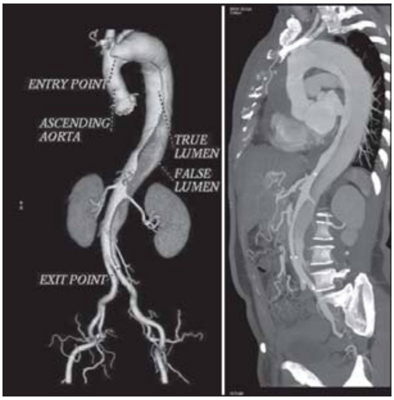

3D volume rendered image with sagittal MPR showing a long segment thoracoabdominal dissection. Note the entry and exit points of this type 3 Debakeys dissection *(For colour version see Fig. 6, Plate 7).*

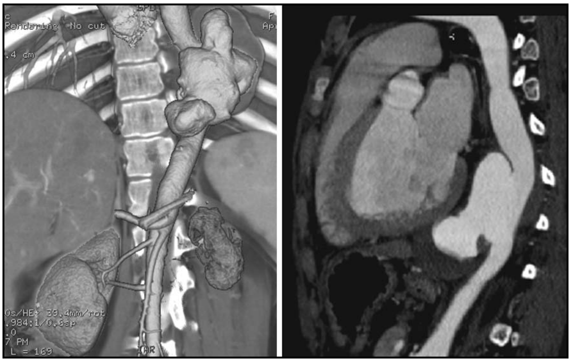

Sagittal MPR with VR image showing a large lobulated saccular aneurysm of the descending thoracic aorta *(For colour version see Fig. 7, Plate 7).*

CT ANGIOGRAM OF EXTREMITIES

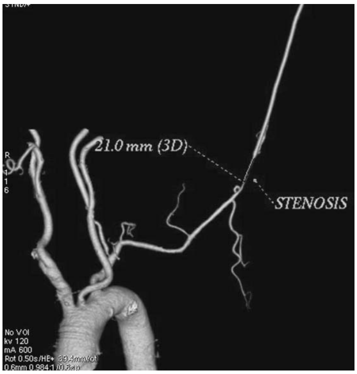

3D VR image showing occlusion of the left brachial artery.
(For colour version see Fig. 8, Plate 8)

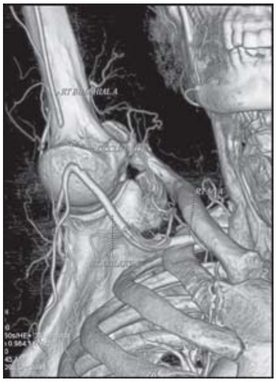

3D VR showing right proximal brachial occlusion.
(For colour version see Fig. 9, Plate 8)

3D VR with MIP images showing occlusion of the right brachial proximal to bifurcation *(For colour version see Fig. 10, Plate 9).*

3D VR with MIP images showing comminuted fracture of tibia and fibula with occlusion of the popliteal artery *(For colour version see Fig. 11, Plate 9).*

CT RENAL ANGIOGRAM

3D MIP with VR image showing left renal pseudoaneurysm post trauma *(For colour version see Fig. 12, Plate 10).*

CT ANGIOGRAM OF SVC OBSTRUCTION

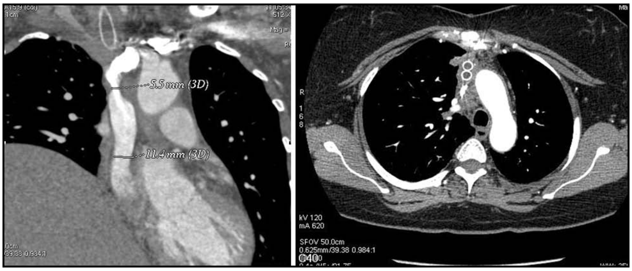

Coronal MIP and axial CECT showing SVC stenosis secondary to fibrosing mediastinitis.

CORONARY CT ANGIOGRAM

3D VR and curved MPR in a young male who had atypical chest pain shows significant narrowing of proximal left anterior descending artery *(For colour version see Fig. 13, Plate 10).*

3D VR and curved MPR in a young smoker showing distal right coronary artery occlusion *(For colour version see Fig. 14, Plate 11).*

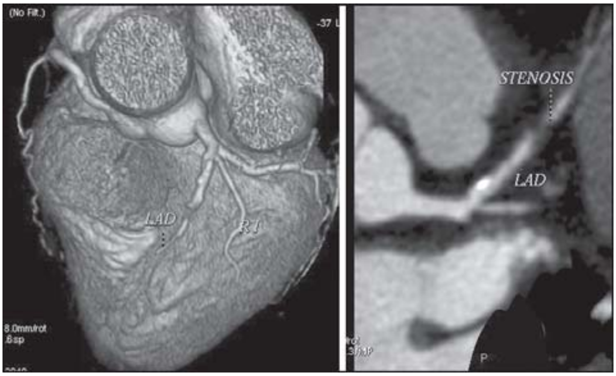

3D VR and curved MPR in a middle aged lady with positive stress test shows short segment occlusion of left anterior descending artery *(For colour version see Fig. 15, Plate 11).*

CT ANGIOGRAM OF BRONCHIAL ARTERIES

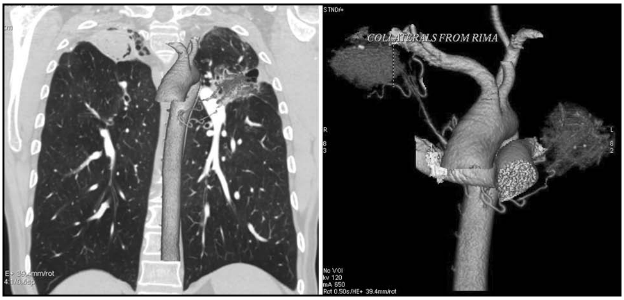

Coronal fusion image with VR image in a patient presenting with hemoptysis- showing bilateral upperlobe cavitary lesions with fungal ball being supplied by the bronchial arteries *(For colour version see Fig. 16, Plate 12).*

CT ANGIOGRAM OF MESENTERIC VESSELS

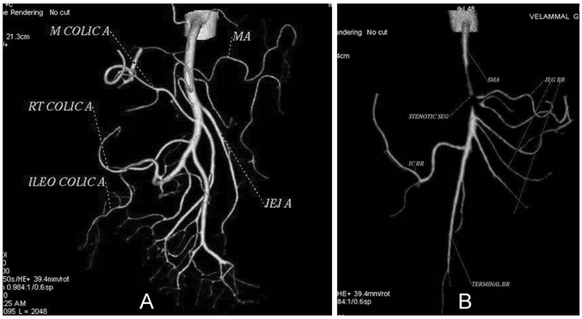

A **B**

(A) 3D VR image showing normal superior mesenteric artery and branches, (B) VR image showing proximal SMA occlusion *(For colour version see Fig. 17, Plate 12).*

Appendix

TRAUMA PEARLS

Initial Survey

1. Primary survey
2. Resuscitation phase
3. Secondary survey
4. Definitive treatment and re-evaluation
5. Transfer if appropriate

Primary Survey

1. ***Airway and Cervical spine***
   - Assess for patency ± removal of foreign material, chin lift, jaw thrust
   - Assume Cx spine injury in all patients with multisystem trauma
   - Lateral Cx spine X-ray ***does not*** exclude all cervical injuries
2. ***Breathing***
   - Exposure of the chest
   - High $FiO_2 > 0.85$

Three commonest traumatic causes of embarrassed ventilation:

i. Tension pneumothorax
ii. Open pneumothorax
iii. Flail chest with pulmonary contusion

3. ***Circulation***
   i. blood-volume and conscious state
      - Skin colour and perfusion
      - Pulse rate and character
   ii. bleeding
      - Esanguinating external haemorrhage should be immediately controlled
      - Occult internal haemorrhage may be difficult to detect/control
      - MAST suit may be appropriate for abdominal/ lower limb bleeding
4. ***Disability*** - overt neurological status
   i. Level of consciousness
      A - alert
      V - responds to verbal stimuli
      P - responds to painful stimuli
      U - unresponsive
   ii. Pupillary size and response to light
5. ***Exposure*** - complete exposure of the patient

Appendix

Resuscitation

1. Supplemental O_2
2. IV access
   i. Minimum of 2x 16 G cannulae
   ii. Blood drawn for X-match, FBE, Coags
   iii. Commence fluid replacement
      - Initially with either balanced salt solution or synthetic colloid use blood if > 2-3 litres in adult with no improvement
   - ***Type-specific*** unmatched, or ***O-negative*** blood acceptable
   - Adequacy of resuscitation judged by physiological parameters
3. ECG monitoring
   - HR, dysrhythmias
4. Urinary catheter
   - Catheter insertion generally contraindicated when,
     i. blood at the external meatus
     ii. blood in the scrotum
     iii. Impalpable, or high riding prostate
5. Naso/oro-gastric tube

Secondary Survey

1. ***Head***
   i. Eyes - pupillary size, response, EOM's, conjunctival haemorrhage
      - visual acuity, lens dislocation, fundi/optic disc changes

   ii. Ears - TM patency, haemorrhage, CSF leak
   iii. Scalp - lacerations, haematoma
2. ***Maxillo-facial trauma***
   - When ***not*** associated with airway compromise, should be deferred to definitive management
   - Mid-face fractures may have fractures of the ***cribriform plate***
3. ***Cervical Spine/Neck***
   - Presume in all patients with blunt maxillo-facial trauma and multisystem trauma
   - Absence of neurological deficit, pain or tenderness ***does not*** exclude significant injury
   - Helmets should be removed with manual in-line stabilisation
   - Penetrating wounds through the platysma require surgical exploration in theatre
4. ***Chest***
   - Anterior, posterior, rib-cage, thoracic spine
   - Bone injury, soft-tissue injury, penetrating injury

- Diminished apical breath sounds may be only sign of pneumothorax
- Soft heart sounds/narrow pulse pressure in tamponade

5. ***Abdomen***
   - Anterior, posterior, lumbar spine
   - Obvious swelling, penetrating injury
   - Consider peritoneal lavage vs CT scan
   - Many centres now trialling emergency ultrasound in assessment
6. ***Rectum***
   - Anal sphincter tone
   - Integrity of rectal wall, presence of fractures
   - Position of prostate
   - Presence of blood
7. ***Fractures***
   - Long bones, joints, digits
   - Pelvis, thoracic cage
   - Spine, cranium
8. ***Neurological***
   - CNS status - AVPU
   - GCS, pupillary responses
   - Motor and sensory evaluation of extremities
   - Vasomotor stability, HR, sphincter tone

9. ***Investigations***
   i. Blood - X match, FBE, MBA, Coags
   ii. X-rays - CXR, AXR, Cx spine
       - pelvis, Tx/Lm spine, long bones
       ± contrast studies
   iii. Diagnostic Peritoneal Lavage
   iv. Ultrasound
   v. CT scan
   vi. Laparotomy

CHEST TRAUMA

Acute Life Threatening Injuries

a. Airway obstruction
b. Tension pneumothorax
c. Open pneumothorax
d. Haemothorax
e. Flail chest
f. Cardiac tamponade
g. Aortic rupture
h. Air embolism - broncho-pulmonary venous fistula
   NB: Chest injuries result in ~ 1/4 trauma deaths, only ~15 percent of such injuries require operative intervention

Appendix

Indications for Intercostal Tube Drainage

1. Pneumothorax
2. Haemothorax
3. Empyema
4. Bronchial rupture
5. Oesophageal rupture
6. Prior to transport in high-risk patients

   Clinical diagnosis for which radiology is used for confirmation:

   a. Respiratory distress
   b. Tracheal deviation
   c. Unilateral diminshed breath sounds
   d. Tympanic percussion note
   e. Pulse paradoxus ± hypotension
   f. Distended neck veins
   g. Cyanosis

MASSIVE HAEMOTHORAX

Usually the result of > **1500 ml** blood in the thoracic cavity

1. Shock
2. Stony dull percussion note
3. Neck veins → ***flat***, due to severe hypovolaemia, or ***Distended***, due to impaired venous return
4. Confirmed by CXR

FLAIL CHEST

Usually 2° multiple rib fractures as a result of blunt trauma if large enough may result in lung pump failure,

1. ***Dominant lesion*** is injury to underlying lung
2. Rarely does flail alone result in respiratory failure
3. Hypoventilation 2° to pain

CXR may show multiple fractured ribs, but may miss costo-chondral separation paradoxical movement may be hidden by splinting in acute setting.

CARDIAC TAMPONADE

Beck's triad,

1. Hypotension
2. Elevated JVP
3. Silent heart

Elevated CVP may be absent with hypovolaemia.

Distended neck veins may be obscured by a cervical collar.

Initial IV resuscitation will elevate CVP and improve CO initially.

Kussmaul's sign, a rise in CVP with inspiration, is a true paradoxical venous pressure abnormality associated with tamponade.

NB: All patients having a positive pericardiocentesis require a thoracotomy.

CHEST TRAUMA - DELAYED MAJOR INJURIES

1. Pulmonary contusion - without flail chest
2. Myocardial contusion - arrhythmias
3. Aortic rupture/haemorrhage
4. Ruptured diaphragm - respiratory failure
5. Ruptured bronchus - bronchopleural fistula
   - pneumothorax
6. Ruptured oesophagus - mediastinitis

PULMONARY CONTUSION

- Most common potentially lethal chest injury seen.
- May be managed with or without intubation, but require observation due to progression over the first 24-48 hrs.

MYOCARDIAL CONTUSION

- Incidence **~ 65 percent** of major blunt chest trauma
- Site affected, a. RV ~ 65 percent b. LV ~ 15 percent c. both ~ 20 percent
- Clinical presentation
  a. Unexplained hypotension
  b. Unexplained elevation of CVP/JVP
  c. Acute cardiac failure
  d. Arrhythmias

e. New murmur - VSD, MV rupture
f. Tamponade

TRAUMATIC AORTIC RUPTURE

Most common major vessel injured following blunt chest trauma common cause of immediate death in MVA, ~ 90 percent fatal at the scene of accident.

Diagnosis

1. CXR may be essentially ***normal***
   - No single finding reliably predicts or excludes significant injury

   i. Widening of the superior mediastinum
   ii. Fractures of the 1st and 2nd ribs
   iii. Blurring of the left margin of the aortic knuckle
   iv. Tracheal shift → right
   v. Left pleural cap effusion
   vi. Elevation and right-shift of the RMB
   vii. Depression of the LMB
   viii. Obliteration of the space between PA and aorta
   ix. Oesophageal deviation (NGT).

Appendix

DIAPHRAGMATIC RUPTURE

NB: High index of suspicion in the patient with major abdominal injuries, modes of ***presentation***,

i. Acute respiratory failure
ii. Bowel sounds in left hemithorax
iii. Peritoneal lavage fluid "disappears", or drains from chest tube
iv. Bowel/NGT in hemithorax on CXR
v. Failure to wean from mechanical ventilation

CXR

a. Loops of bowel in ***left hemithorax***
b. "pseudo-haemopneumothorax" = air/fluid level of stomach
c. Persistent elevated left hemidiaphragm
d. NG tube in left hemithorax

NB: May be ***mimicked*** by (misinterpreted as),

i. Elevated left hemidiaphragm
ii. Acute gastric dilatation
iii. Loculated pneumothorax
iv. Subpulmonic haematoma

TRACHEOBRONCHIAL TREE INJURIES

Laryngeal Injury

a. History of injury
b. May be minimal external tissue damage
c. Hoarseness
d. Subcutaneous emphysema
e. Crepitus

Bronchial Rupture

a. Sites
   i. Lower trachea ~ 80 percent transverse
   ii. Major bronchus - spiral
   iii. Post. tracheal wall - vertical

Oesophageal Rupture

Clinical presentation,
a. Penetrating, most common, or severe closed chest trauma
b. Retrosternal pain
c. Dysphagia
d. Haematemesis
e. Cervical emphysema

f. CXR: - left pleural effusion, haemothorax
   - widened mediastinum
   - mediastinal emphysema, air/fluid level
   - cervical emphysema
   - hydropneumothorax/pneumothorax
g. Pleural aspirate - pH < 6.0
   - bloody fluid, high WCC
   - high amylase

COMA: CAUSES OF RESPIRATORY FAILURE

a. Airway obstruction
b. Aspiration
c. Acute neurogenic pulmonary oedema
d. Post-obstructive pulmonary oedema
e. Thoracic injuries
   i. Tracheobronchial disruption
   ii. Pulmonary contusion
   iii. Haemothorax/pneumothorax
   iv. Flail chest
   v. Diaphragmatic disruption
f. Acute gastric dilatation
g. Cervical cord trauma
h. Central hypoventilation

ABDOMINAL TRAUMA

Peritoneal Lavage

a. Sensitivity ~ 95-98 percent
b. Specificity ~ 85 percent
c. Positive result
   - Renal injury

Indications

a. Multiple trauma patient in whom abdominal examination is,
   i. Equivocal
   ii. Unreliable - CHI, intoxication, cord injury
   iii. Impractical - prolonged X-Rays, angiography
      - Requiring GA
b. Unexplained fluid requirements in resuscitation
c. Penetrating injuries - including lower thoracic
d. Gunshot wounds

Contraindications

a. Full bladder
b. Pregnancy
c. Recent abdominal surgery
d. Obvious signs of intraperitoneal haemorrhage/ infection

NB: The only ***absolute contraindication*** is an existing indication for laparotomy.

Complications

a. Haemorrhage
b. Intestinal perforation
c. Bladder perforation
d. Infection

Peritoneal Lavage - Technique

a. Empty bladder, sterile technique, IV access
b. Dialysis catheter introduced into pelvis via sub-umbilical incision
c. Aspiration for frank blood
d. 1000 ml of normal saline introduced over 5 minutes + ballotment
e. Fluid drained sent for,
   i. red and white blood cell counts
   ii. urgent gram stain and culture
   iii. amylase
   iv. ? cytology

ABDOMINAL CT SCANNING

- Suggested as a substitute for DPL in haemodynamically stable patients.
- Criticism of DPL is indication for laparotomy in cases of minor liver laceration.

GENITOURINARY TRACT

Blunt Trauma

Increased incidence of injury with,

a. Renal
   i. Back/flank haematomas, ecchymoses
   ii. Fractures of lower ribs
   iii. Fractures of spinal transverse processes

b. Bladder/urethra
   i. Perineal haematomas
   ii. Anterior pelvic fractures

c. Overt signs of lower tract injury
   i. Blood at the urethral meatus
   ii. Inability to void

- Urethral disruptions are divided into:

a. Posterior - above the urogenital diaphragm
   - Usually multisystem trauma, pelvic fractures

b. Anterior - below the urogenital diaphragm
   - Usually starddle injuries and isolated

- Imaging techniques

1. IVP
    - Unilateral non-function - congenital absence, previous nephrectomy
        - Massive parenchymal shattering
        - Vascular pedical disruption
2. Urethrography
    - Should be performed prior to CUD in all suspected urethral tears
3. Cystography
4. CT scan

Pelvic Fractures

- Open pelvic fractures → ***mortality* > 50 percent**
- Rectal and genital injuries should be suspected in all major fractures
- DPL should be performed, preferrably from ***above*** the umbilicus, due to extension of haematoma
    a. Negative DPL - reliably excludes major intra-peritoneal bleeding
    b. Positive DPL ~ 15 percent FP, due to leaking into the peritoneum
- A MAST suit may be used if there is haemodynamic instability

- Continued bleeding then become a therapeutic dilemma,
  a. If DPL is grossly positive, then laparotomy indicated to exclude co-existent abdominal pathology
  b. ***Arteriography/embolization*** may be life-saving for uncontrolled haemorrhage.

HEAD TRAUMA

Head injury is associated with,

a. ~ 50 percent of all trauma deaths
b. ~ 60 percent of MVA deaths

Def'n: coma is defined as,

1. No eye opening = 1
2. Not obeying command = 1-5
3. No word verbalisation = 1-2
   - Virtually all patients with GCS < 8 and
   - Most with GCS = 8 are comatose

Def'n: head injury is arbitrarily divided according to GCS as,

1. Severe HI GCS < 9
2. Moderate HI GCS = 9-12
3. Minor HI GCS > 12

Other factors considered as severe HI, despite GCS,

a. Unequal pupils > 1 mm difference
b. Unequal motor response
c. Open HI - CSF leak, exposed brain tissue
d. Neurological deterioration
e. Depressed skull fracture

- A change in GCS ≥ 2 represents clear deterioration, ≥ 3 major deterioration requiring immediate
- Assessment and therapy
- Other factors of concern,
    a. Increased severity, or unusually severe headache
    b. Unilateral increase in pupil size
    c. Unilateral onset of weakness

Imaging Techniques

a. CT scan
    - Examination of first choice in all but trivial injuries

b. SXR
    - Limited value in early management, except in penetrating injuries

c. Examination with limited/no role in acute head injury
    i. LP
    ii. EEG
    iii. Isotope scanning

Skull Fractures

a. Linear, non-depressed
   Across vascular arterial grooves or suture lines increases the risk of ***extradural haematoma***
b. Depressed
   Increased risk of sequelae (eg seizures) in depressed > thickness of skull
c. Open
   Early operative intervention, elevation and removal of fragments and closure of the dura
d. Basal skull fractures
   Internally compound, and loss of CSF may be occult into sinuses
   Factors suggestive of diagnosis,
   i. Battle's sign - mastoid ecchymoses
   ii. Raccoon eyes - bilateral periorbital ecchymoses - associated with cribiriform plate fracture
   iii. CSF leak - rhinorrhoea, otorrhoea
   iv. Haemotympanum

Diffuse Brain Injury

a. ***Concussion***

- Is a brain injury accompanied by brief loss of neurological function

- Various neurological abnormalities may be described, however, these have usually resolve by the time a tertiary institution is reached
- ***Any*** neurological abnormality observed in a patient ***should not*** be attributed to concussion
- Rule of thumb is that if the patient has been unconscious for > 5 minutes then they should be observed for 24 hrs

b. ***Diffuse axonal injury***

- Characterised by prolonged coma, lasting days to weeks
- Overall mortality ~ 30 percent
- Autonomic dysfunction, fever, hypertension, sweating, etc is common.

Focal Injuries

a. Contusions
b. Haemorrhages
c. Haematomas

Meningeal Haemorrhage

1. Extradural haemorrhage
   - Most commonly middle meningeal artery, rarely dural sinus
   - Usually 2° linear fracture of parietal/temporal bones
   - Relatively rare ~ 0.5 percent of unselected HI

2. Subdural haemorrhage
   - Much more common than extradural ~ 30 percent of severe HI
   - Most commonly rupture of ***bridging veins***, less often cortical arteries or brain
   - Underlying primary brain injury is often severe
   - Poor prognosis → mortality ~ 60 percent
   - Recent studies suggest some improvement of outcome with early evacuation
3. Subarachnoid haemorrhage
   - Blood in CSF → meningeal irritation, headache, photophobia, etc.
   - LP not required → CT scan

Parenchymal Haemorrhage

1. Intracerebral haematomas
2. Impalement injuries
3. Bullet wounds.

SPINAL TRAUMA

Demographics

a. Age ~ 70-80 percent are between **11-30 yrs**
b. Sex ~ 2/3 are ***males***

c. ***Mortality*** ~ 30 percent die before reaching hospital
   1. Flaccid areflexia
   2. Flaccid rectal sphincter
   3. Ability to flex, but ***not extend*** the elbow
   4. Grimaces to pain above, but not below the clavicle
   5. Hypotension with bradycardia and dilated veins
   6. Priapism

Vertebral Assessment

a. Usually associated with pain and tenderness
b. Less often palpable step-deformity
c. Oedema/ecchymoses
d. Tracheal tenderness/deviation - retropharyngeal haematoma
e. Muscle spasm ± head tilt

Neurological Assessment

a. Motor power
b. Tone
c. Reflexes
d. Sensory deficit
   - Light touch is conveyed in both lateral and posterior columns and may be the only modality preserved in incomplete injuries.

- Sparing of sensation in the ***sacral dermatomes*** may be the only sign of incomplete injury.
- Evaluation of sacral sparing should include sensory perception and voluntary contraction of the anus.

e. Autonomic dysfunction - bladder/rectal control, priapism.

Neurogenic and Spinal Shock

1. ***Neurogenic shock***
   - Hypotension associated with high thoracic and cervical injuries
   - Hypotension, bradycardia and dilated veins → "relative hypovolaemia"
   - Atropine may be used to Rx bradycardia.
2. ***Spinal shock***
   - Refers to neurological function of the spinal cord following injury
   - "Shock" may result in almost total non-function despite viability of the cord
   - Produces flaccid paralysis, cf. normal spasticity, brisk reflexes and ↑ plantars.

Appendix

Fractures/Dislocations

1. ***C1 Atlas***
   - Usually involves a blow-out of the ring → ***Jefferson*** fracture associated with axial load
   - 30 percent have associated C2 fracture
   - Usually ***not*** associated with cord injury
   - They are unstable and require immediate immobilization.
2. ***C2 Axis***

i. Dislocation
   - Odontoid may be displaced posteriorly into the spinal canal
   - Injury to the transverse ligament, between odontoid and anterior arch of C1
   - Consider whenever C1-arch to odontoid distance > **5 mm**
   - Displacement can occur without injury → Steel's rule:
   - "1/3 of the area in the atlas is occupied by odontoid, 1/3 by spinal cord".

ii. Odontoid fractures

Type I: above the base and stable

Type II: through the base and usually unstable

Type III: extends into the vertebral body

NB: In children under 6 yrs the epiphysis may appear as a fracture line cf. type II fractures.

iii. Posterior element fractures → ***"hangman's*** fracture"
  - Posterior elements damaged by flexion and distraction unstable.

3. ***C3-C7***
   - Assess distance from anterior aspect of C3 to pharyngeal shadow → prevertebral thickness < 5 mm
   - Increased thickness "without" fracture classically seen with minimally displaced C2 fracture
   - "Rule-of-thumb" for prevertebral haematoma is the distance to the air-shadow should be < ½ the vertebral body thickness
   - Radiological evidence identifying an unstable fracture,
     i. ***Disruption*** of all of either anterior or posterior elements
     ii. ***Over-riding*** of a superior vertebral body > **3.5 mm**
     iii. ***Angulation*** between vertebral bodies > **11°**
4. ***Facet dislocations***
   - Unilateral facet injury → vertebral displacement ~25 percent of body width
   - Bilateral facet injury → vertebral displacement > 50 percent of body width
   - Malalignment of spinous processes on AP film
   - Bilateral dislocations frequently unstable.

Appendix

PAEDIATRIC TRAUMA

- Ratio of blunt:penetrating trauma highest for paediatric group
- MVA's and falls account for ~ 80 percent of trauma
- ***Multisystem*** injury is the rule, rather than the exception.

Unique Characteristics

1. Smaller size - greater force per unit area
2. Skeletal immaturity
   - Soft bones with active growth centres can absorb large amount of energy without fracture
   - Higher incidence of internal organ damage without overlying fracture
   - Includes spinal column → SCIWORA
   - Open sutures < 18 months
3. Surface area
   - Thermal energy loss higher
   - Absorption of toxins higher
   - Systemic effects of burns greater
4. GCS modified for age
5. Higher incidence of:
   i. Seizure activity
   ii. Mass lesions
   iii. White matter tears - frontal and temporal lobes - especially infants < 6 months
   iv. Subdural haematomas - especially NAI

6. Major blood loss with ***hypotension*** may be ***concealed***
7. IV access often more difficult
8. Acute gastric distension → NG tube
9. Psychological immaturity
10. Long-term effects
    - Growth and deformity
11. Equipment
    - Specific equipment required → size for age ***not*** small adults.

Chest Trauma

a. Majority blunt
b. Underlying ***pulmonary contusion***/haemorrhage most common significant injury
c. Tension pneumothorax/haemothorax are less common cf adults, but may be rapidly lethal if unrecognised
d. Injuries relatively rare in paediatric group,
    i. Fractures ribs
    ii. Diaphragmatic rupture
    iii. Injury to great vessels

Abdominal Trauma

NB: All should have stomach decompressed by oro/nasogastric tube.

a. High incidence of visceral injury
b. More difficult to assess cf adults
c. Limited role for DPL → ***CT scan***
   - CT must be - immediately available
     - not delay diagnostic algorithm
     - suit must have resuscitation facility
d. Majority of solid visceral injuries are managed ***conservatively*** but require adequate observation
e. Indications for operating on spleen/liver trauma,
   i. Failure to respond to resuscitation
   ii. Continued major haemorrhage > 40 ml/kg/24 hrs
   iii. Suspicion of associated hollow visceral injury
   iv. Severe concomitant HI, where haemodynamic instability is deleterious
f. Many liver/spleen injuries can be repaired, rarely perform ***splenectomy.***

Extremity Trauma

a. Presence of growth plates makes assessment difficult. X-ray of the opposite limb often useful.
b. Blood-loss associated with long-bone and pelvic fractures is proportionately more significant.
c. ***Physeal*** fractures classified by Salter-Harris
   i. Type I - linear through growth plate
   ii. Type II - cf. type I, plus small chip of metaphysis

iii. Type III - through growth plate and epiphysis
iv. Type IV - through both metaphysis and epiphysis
v. Type V - compression fractures
   - Types I and II have best prognosis for normal growth.
   - Type V has worst prognosis and difficult to spot on X-ray.

d. Greenstick fracture - fracture of cortex only
   - most require reduction
e. Buckle fracture - angulation without cortical fracture
f. Supracondylar fracture
   - High propensity for neurovascular injury
   - High incidence of growth deformity.

Head Trauma

a. Children < 3 years have worse outcomes following severe HI
   - Cf. older children who generally recover better than adults
b. Small children may develop hypovolaemic shock 2° head injury alone, or associated scalp laceration
c. Children < 18 months with open sutures have increased tolerance of expanding intracranial masses. Check for fontanelle bulging and suture diastasis

d. Vomiting is a common response to injury and may, or may not, equal raised ICP
e. Seizures occurring shortly after injury are usually self-limiting recurrent seizures require Ix and Rx
f. Focal lesions are less common
g. Generalised oedema and raised ICP is more common
h. GCS, verbal score modified for age,
   i. Appropriate words
      - Social smile
      - Fixes and follows = 5
   ii. Cries but consolable = 4
   iii. Persistently irritable = 3
   iv. Restless, agitated = 2
   v. None = 1
i. Indications for ICP monitoring in children
   i. GCS < 5, or motor scores < 3
   ii. Where raised ICP is known, or likely to develop, and signs are masked by neuromuscular paralysis
   iii. Multiple associated injuries, where CT scanning delayed.

   ICP monitoring/management ***does not*** improve outcome in global ischaemic events near-drowning victims with ↑ ICP/↓ CPP have poor prognosis, and maintenance of 'normal' ICP does not correlate with outcome.

j. Child drug doses
   i. Diazepam ~ 0.25 mg/kg
   ii. Phenytoin ~ 15-20 mg/kg
   iii. Mannitol ~ 0.5-1.0 g/kg

Spinal Trauma

Paediatric spinal trauma is relatively rare → ~ 5 percent of all spinal injuries of children with severe trauma ~ 5 percent will have a cervical spine injury. Injuries will occur at more than one spinal level in ~ 16 percent of cases the commonest causes are:

a. Road trauma - MVA, pedestrian, cyclist
b. Falls - especially diving

   Anatomical differences include:
   a. Interspinous ligaments and joint capsules are more flexible
   b. Uncinate articulations are poorly developed and slide forward
   c. The facet joints are flat
   d. The vertebral bodies are wedged anteriorly and slide forward with flexion
   e. The head is relatively large

→ greater angular momentum can be generated with flexion/extension normal radiological variations include:

a. Anterior displacement of C2 on C3 →
   i. ~ 40 percent of children < 7 yrs
   ii. ~ 20 percent of children ≤ 16 yrs
   iii. ± ≥ 3 mm movement on flexion/extension
b. Increased distance between the dens and anterior arch of C1 ~ 20 percent of children
c. Skeletal ***growth centres*** may resemble fractures
d. Basilar ***odontoid synchondrosis*** appears as a radiolucent line at the base of the dens (especially ≤ 5 years). Spinal cord injury without radiographic abnormality, ***SCIWORA*** is almost unique to the paediatric age group
   - ~ **20-60 percent** of all SCI
   - ~ 30-50 percent of these the lesion is complete

SCI in the first decade of life is,

a. Almost exclusively at C1/2
b. Either subluxation or SCIWORA and severe cord injury
c. Rarely associated with fractures

A high proportion of children who die in MVA's, or suffer cardiorespiratory arrest prior to reaching hospital have cord trauma above C3, particularly at the ***cervico-medullary junction.*** This is difficult to diagnose in the unconscious patient, signs including:

a. Flaccid immobility and areflexia
b. Hypoventilation with paradoxical chest movement
c. Apnoea and rhythmic flaring of the alae nasi (above C3)
d. Hypotension with - inappropriate bradycardia
   - – peripheral vasodilatation
   - ± priapism

Spinal Shock

The syndrome of spinal shock occurs more commonly in children,

a. SCI lesion resolves after 2-3 days
b. Progressive return of reflexes - bulbocavernous and anal first
c. Incomplete lesions may then become apparent
   i. Brown-Sequard hemisection
   ii. Anterior cord lesion
   iii. Central cord lesion
d. Physical
e. Sexual and emotional abuse
f. Deprivation of medical care and nutrition. Children are also intentionally poisoned, and endure the consequences of inadequate supervision. Diagnosis of children who suffer from abuse or neglect is difficult.

NAI should be suspected where:
a. An injury is unexplained
b. The history is not consistent with the type of injury
c. It is alleged that the injury was self-inflicted
d. Relatives delay in seeking medical aid
e. There are repeated suspicious injuries
   - The history is rarely volunteered by the child
   - The pattern of physical findings can be helpful

a. Head injury - skull fractures
   - subdural haematomas
b. ***Retinal haemorrhages*** occur with head shaking, but also have other causes
c. Bruises and scars on the back and buttocks in different stages of development and of unusual shapes
d. Burns from cigarettes or forced immersion in hot water
e. Overt bone fractures or ***healing fractures***
f. Long-bone fractures in children < 3 years
g. Injury to genital or perianal areas.

When non-accidental injury is suspected, referral to a specialised child protection unit to enable appropriate counselling and intervention is helpful. Safety of siblings must be considered.

Index

Index